IEEE Access
Multidisciplinary | Rapid Review | Open Access Journal

Received February 10, 2020, accepted February 22, 2020, date of publication February 28, 2020, date of current version March 16, 2020.

*Digital Object Identifier 10.1109/ACCESS.2020.2977167*

# A Survey of Performance Enhancement Techniques of Antipodal Vivaldi Antenna

**AMRUTA S. DIXIT AND SUMIT KUMAR**
Electronics and Telecommunication Department, Symbiosis Institute of Technology (SIT), Symbiosis International (Deemed University) (SIU), Pune 412115, India

Corresponding author: Sumit Kumar (er.sumitkumar21@gmail.com)

**ABSTRACT** The increasing proliferation of advanced devices for UWB, 5G communication, micrometer-wave, and millimeter-wave communication demands an antenna which can handle huge data rates, provides high gain and stable radiation pattern as a panacea of most of the current wireless communication problems. Many different antenna designs have been proposed by the researchers but, Antipodal Vivaldi Antenna (AVA) has drawn the attention of most of the researchers because of its high gain, wide bandwidth, less radiation loss, and stable radiation pattern. Different methods are presented to make AVA more compact while maintaining the performance of an antenna to an acceptable level. These different methods are substrate choice, flare shape, slots, and feeding connectors. Also, AVA performance can be enhanced by incorporating corrugation, dielectric lens, patch in between two flares of AVA, balanced AVA (BAVA), metamaterial, computational intelligence (CI), and AVA array. The AVA performance enhancement techniques modify the electrical and physical properties of an antenna which in turn improves its performance. A large number of performance enhancement methods of AVA design have been proposed, however, no comprehensive study exists to categorize these performance enhancement techniques and outline their concepts, advantages, disadvantages, and applications. So, in this paper, we have attempted to outline all methods available for enhancing and optimizing the parameters of AVA. Additionally, to validate some of the important performance enhancement methods, they are incorporated in the basic conventional AVA design and further simulation results are obtained for the same which are in line with the surveyed literature. Each method is explained in detail by incorporating its key points, merits, and demerits. Moreover, illustrations from the literature are given to demonstrate improvement in the parameters as a result of applying a particular performance enhancement technique.

**INDEX TERMS** Antipodal Vivaldi antenna (AVA), AVA array, balanced antipodal Vivaldi antenna (BAVA), corrugations, dielectric lens, metamaterial, parasitic patch, slots.

## I. INTRODUCTION

Current wireless devices demand wide bandwidth, high data rate, and more capacity. Antipodal Vivaldi Antenna (AVA) is a promising solution to different daunting tasks present in the current communication systems. Recent development shows that AVA can be widely used in many applications like an ultra-wideband (UWB), radar, 5G communication devices, to identify voids in the concrete beam (civil), micrometer and millimeter-wave applications as shown in figure 1. Dr. P. J. Gibson introduced the Vivaldi antenna in IEEE 9th European Microwave conference in1979 titled **The Vivaldi Aerial** [1]. This Vivaldi antenna is linearly polarized and can operate at wide bandwidth with high and constant gain. This designed Vivaldi antenna gave 10 dB gain and −20 dB sidelobe level over 2 to 40 GHz frequency range [1]. Vivaldi antenna is also called as a tapered slot antenna because of its structure. Dr. Gibson was much more interested in music. His favorite music composer was Antonio Vivaldi who was from the Baroque period (early $17^{th}$ to mid $18^{th}$ century). Vivaldi was the great violin composer. The shape of the antenna designed by Dr. Gibson resembles the violin structure and he was a great fan of Antonio Vivaldi. Hence Dr. Gibson gave Vivaldi name to his antenna. The basic design structure of the Vivaldi antenna is given in figure 2(a). Vivaldi antenna comes under aperiodic and gradually scaled end-fire antenna. Theoretically, the Vivaldi antenna can operate at an overall frequency range with constant beamwidth [1], [2].

The associate editor coordinating the review of this manuscript and approving it for publication was Yuan Yao.


**FIGURE 1.** Applications of AVA.

Practically Vivaldi antenna's bandwidth, beamwidth, side, and back lobes depend on feeding microstrip line, size, and shape of Vivaldi flare. As shown in figure 2(a), the Vivaldi antenna consists of two flares that act as ground radiators and the feed line is present on the opposite side of the substrate.

To reduce the beamwidth, sidelobes, back lobe and return loss Dr. Gazit introduced AVA in 1988 [3]. Two flares of Vivaldi are antipodal as they are present on the opposite side of the substrate. The top flare (upper patch) acts as a conductor and the bottom flare (lower patch) acts as a ground. Both the flares are mirror images of each other. Nowadays, AVA is used by many researchers as compared to Vivaldi because of its high gain, high efficiency, low return loss, wide bandwidth, reduce sidelobe levels, it can operate at high frequencies, and provides stable radiation pattern. The basic structure of the AVA is shown in figure 2(b).

The dimensions of AVA length (L), width (W) and tapered slots (Y) are calculated by equations 1 to 5 [6].

Length (L) of Vivaldi antenna should be greater than half of wavelength ($\lambda$)

$$L > \frac{\lambda}{2} \tag{1}$$

where, $\lambda$ is maximum operating wavelength.

Width (W) of Vivaldi antenna should be greater than one fourth of wavelength

$$W > \frac{\lambda}{4} \tag{2}$$

Equation of tapered slot is given by

$$Y = \pm(C_1 e^{ax} + C_2) \tag{3}$$

where $C_1$ and $C_2$ are given by,

$$C_1 = \frac{y_2 - y_1}{e^{ax_2} - e^{ax_1}} \tag{4}$$

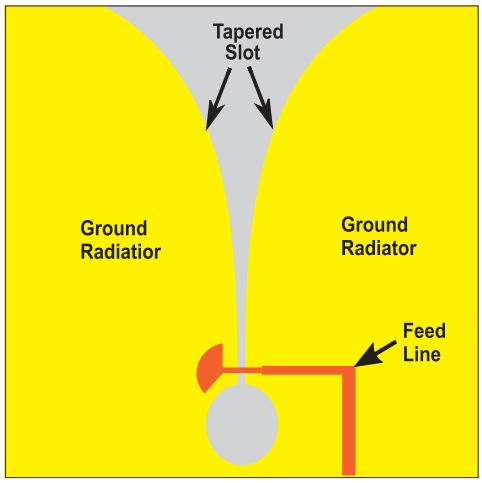


(a) Structure of Vivaldi antenna [4]

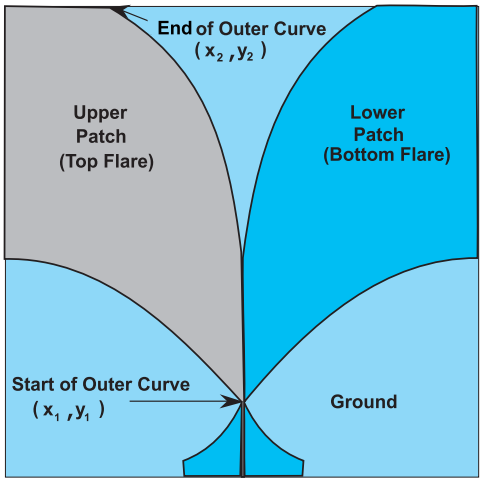


(b) Structure of antipodal Vivaldi antenna(AVA) [5]

**FIGURE 2.** Antenna Structures.

$$C_2 = \frac{e^{ax_2} y_2 - e^{ax_1} y_1}{e^{ax_2} - e^{ax_1}} \tag{5}$$

Here, $C_1$ and $C_2$ are constants; 'a' is a rate of increase of exponential curve. $x_1$, $y_1$, $x_2$, and $y_2$ are start and end points of exponential curve as shown in figure 2(b).

Figure 3 depicts the various advantages of AVA. Few examples of advantages of AVA are taken from the literature and are listed below:

- **High Gain:** AVA and its array structure can provide the gain above 18dB [7] and 23dB [8] respectively.
- **Improved Return Loss:** AVA improves return loss very effectively up to −50dB [9], [10].
- **High Efficiency:** As a result of improved return loss, we get good impedance matching for increasing AVA efficiency. AVA efficiency goes beyond 90% [11], [12].
- **Enhanced Beamwidth:** AVA reduces beamwidth to a very low level to increase its gain. For example, in [11] beamwidth is reduced to 17.6° at 40GHz and in [13] beamwidth is 24.6° at 35 GHz.

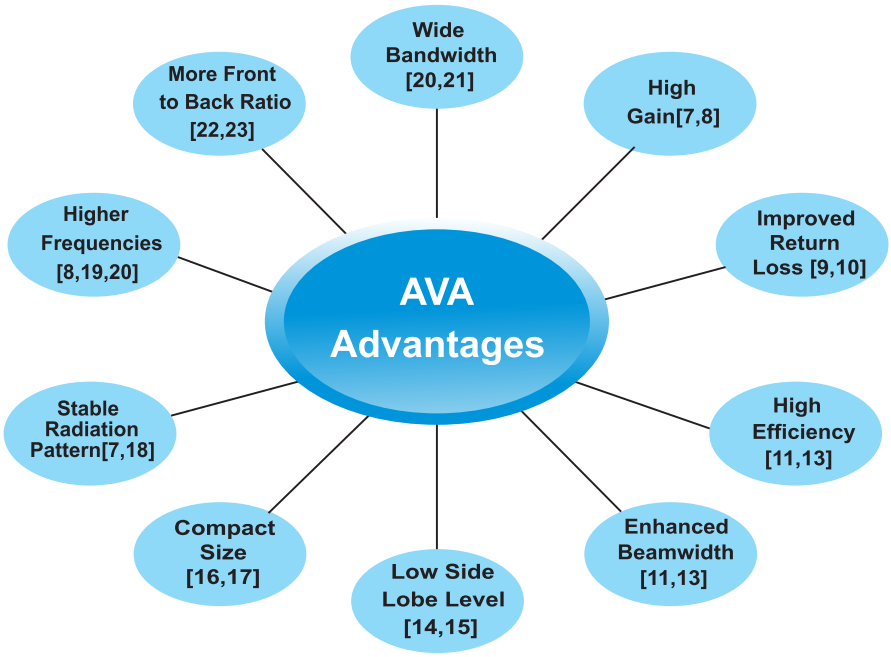


**FIGURE 3.** Advantages of AVA.

- **Low Sidelobe Level:** It also reduces the sidelobe level and back lobe levels below −13dB [14], [15].
- **Compact Size:** By using various miniaturization techniques, AVA can be made compact of size nearly 30mm × 30mm [16], [17].
- **Stable Radiation Pattern:** The radiation pattern is symmetric and almost not dependent on frequency [7], [18].
- **Higher Operating Frequencies:** AVA operates at high frequencies ranging from 1 GHz to 100 GHz [8], [19], [20]. It provides wide bandwidth of 1:10 [21] or the bandwidth of 150 GHz [20].
- **More Front to Back Ratio:** It maintains front to back ratio to a high level of above 30dB [22], [23].

BAVA gives better gain than the conventional AVA but, the design complexity, antenna size, and fabrication cost is higher. Hence, AVA is preferred in comparison to BAVA provided its gain can be increased. In order to increase the gain, several researchers are working on the gain enhancement techniques. This motivated us to survey the performance enhancement methods of AVA like corrugation, metamaterial, array, dielectric lens, and parasitic patch to enhance the gain and other parameters of conventional AVA which already has advantages like simplicity, miniaturization, and low fabrication cost.

The paper structure is as follows: Section 2 includes AVA performance enhancement methods, section 3 validates some of the important enhancement methods discussed in section 2, and section 4 concludes the paper.

## II. PERFORMANCE ENHANCEMENT TECHNIQUES FOR AVA

There is a plethora of investigation on AVA performance enhancement. AVA larger size may render it to be used in compact communication devices. But, AVA can be made compact with required specification by incorporating metamaterial, substrate having low loss tangent and low relative permittivity, shape of flare of AVA, slots with different position and widths, corrugation, dielectric lens, by adding patch in between two flares, different types of connectors for feeding, Balanced AVA, AVA array, multiple input and multiple outputs, and computational intelligence techniques. Different methods to enhance the performance of Antipodal Vivaldi Antenna (AVA) are described in detail in this section. Each technique is explained with the help of AVA designs from recent papers. The performance of every technique is compared in terms of antenna gain, return loss, dimension and operating frequency range. Figure 4 shows the different methods of AVA performance enhancement techniques.

Computational intelligence techniques like Particle Swarm Optimization (PSO), multi-objective PSO(MOPSO), and multiobjective genetic algorithm (MOGA) can be used to decide dimensions of an antenna to optimize the different parameters of an antenna. PSO is popularly used in AVA to reduce transient distortion, cross-polarization and reflection coefficient [24]. Multi-objective PSO is applied to AVA array to enhance sidelobe level and mutual coupling in [25], [26]. A compact balanced antipodal Vivaldi antenna can be implemented by using PSO [27]. AVA becomes a good choice for millimeter and ultra-wideband applications if its size can be reduced.

The metamaterial is employed in an antenna design due to its special electromagnetic characteristics which cannot be found in natural materials. There are different types of metamaterials like an electromagnetic, single negative, double negative, electromagnetic bandgap, isotropic, anisotropic,

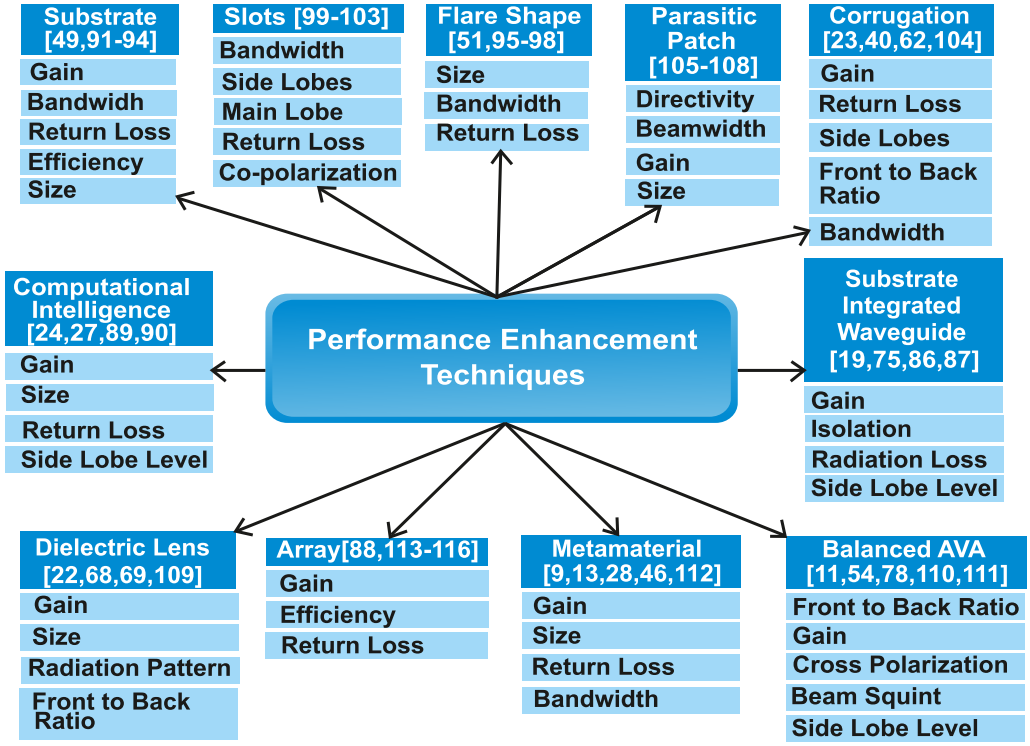


**FIGURE 4.** AVA parameters and their enhancement techniques.

chiral, terahertz, photonic, tuneable, frequency selective surface-based, and nonlinear metamaterial. The metamaterial is not available in nature; they have to be designed manually with the help of two or more natural materials. There are many more advantages of using metamaterial in antenna design, for example, hike in gain and bandwidth, noticeable reduction in the size of an antenna, negligible surface waves, and fewer sidelobes. Recent developments show that single negative, double negative and anisotropic metamaterials are used in AVA antenna design [5], [9], [28]–[31].

Different types of substrates are available in the market. A substrate with low loss tangent and low relative permittivity is desirable. Electric permittivity is the potential of the substrate to store the electrical energy in an electric field. A vacuum has the lowest permittivity. Relative permittivity is the factor by which the electric field between the charges is decreased relative to the vacuum. If the relative permittivity of the substrate is high then the magnitude of the electric field reduces considerably within the volume of the substrate. This reduces the gain of an antenna. Hence a substrate with low relative permittivity should be selected. The loss tangent of a substrate is the indicator of power loss due to its material. Low loss tangent means low power loss. As low power loss is required for an antenna operation, a substrate with a low loss tangent should be selected. These losses can be further reduced by using Substrate Integrated Waveguide (SIW) [32].

Research on AVA shows that AVA flares can be designed with different shapes like Chebyshev [33], wide elliptical [34], leaf structure [35], binomial [36], fractal [37], etc. to enhance the performance of an antenna. Also, circular [38] or rectangular slots [39] at different positions are designed on AVA flare to increase the bandwidth of AVA. AVA provides low gain at low frequency. This drawback can be overcome by using corrugation [40]. The corrugation on the outer edges of a flare of AVA helps in improving the low-frequency performance of AVA. Corrugations can be of sine, straight rectangular, slant rectangular or triangular shape. The dielectric lens transmits radiation in one direction. Thus increasing directivity and gain of an antenna [41]. The dielectric lens can be made up of the same substrate material or different materials. Different shapes of the dielectric lens are elliptical, circular, trapezoidal or rectangular. An extra patch can be made in between two flares to reduce the cross polarization [42]. This in return increases the gain and reduces reflection losses of an antenna. Impedance matching is very important to reduce the loading effect of an antenna. Hence an efficient feeding network is required to be implemented. The various feeding methods are microstrip line, electromagnetically coupled feed, and aperture coupled feed. The parallel microstrip feed line provides a good impedance match and hence improves return loss as compared to the exponential curve microstrip line [43]. As compared to a single antenna, multiple antennas give much better performance. Hence, the gain, bandwidth, and efficiency can be enhanced by using AVA array [44] at the cost of a larger size.

It is not possible to cite each and every published paper on AVA. But, we have covered all AVA performance

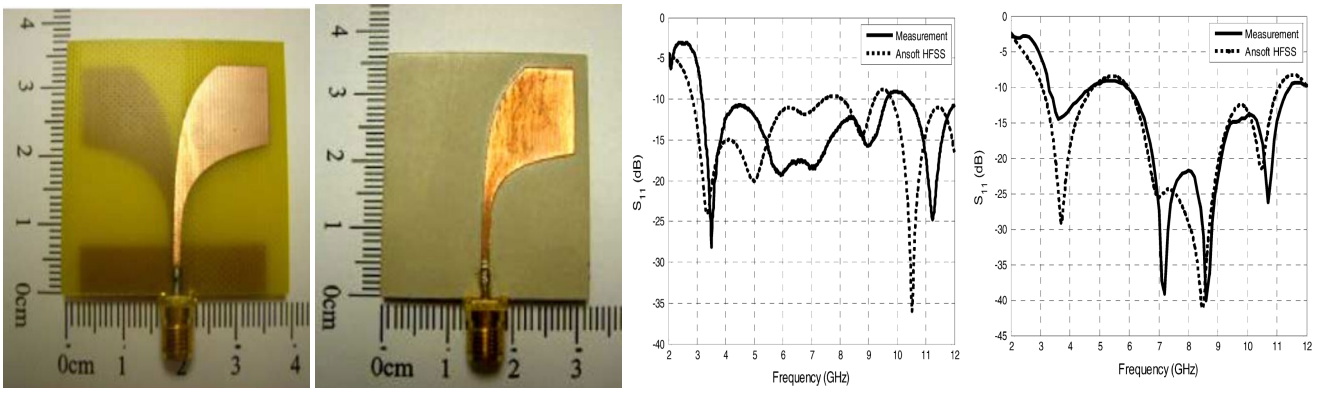


(a) Top view of AVA on FR4 (b) Top view of AVA on RO3006 (c) S11 of AVA on FR4 (d) S11 of AVA on RO3006

**FIGURE 5.** Comparison of FR4 and RO3006 substrates [49].

**TABLE 1.** Comparison of antipodal Vivaldi antennas with different substrate materials.

| Ref. | Substrate | Permittivity | Loss Tangent | Thickness | Size ($mm^2$) | Return Loss (dB) | Gain (dB) | Frequency (GHz) | Applications |
|---|---|---|---|---|---|---|---|---|---|
| [45] | FR-4 | 4.4 | 0.02 | 1.6 | 80 x 60 | -30 | 2-8 | 3.1-10.6 | UWB |
| [46] | F4BM265 | 2.65 | 0.001 | 1 | 130 x 80 | -27 | 2.27-14 | 1.13-12 | UWB |
| [47] | RO3006 | 6.15 | 0.002 | 1.28 | 45 x 60 | -30 | 2.2-6.8 | 1.7-11 | UWB |
| [48] | RO5880 | 2.2 | 0.009 | 0.508 | 171 x 202 | -42 | 4-8.5 | 0.67-6 | Construction |
| [10] | RO4003 | 3.38 | 0.0027 | 0.508 | 40 x 60 | -50 | 8-15 | 3.4-40 | $\mu$Wave |
| [49] | RO3006 | 6.15 | 0.002 | 1 | 39.4 x 34.6 | -40 | -2-5.2 | 3.1- 10.6 | UWB |
| | FR-4 | 4.4 | 0.02 | 1.4 | 40.16 x 42.56 | -28 | -1-5 | 3.1- 10.6 | |

enhancement techniques including their key points, the effect on antenna parameters, advantages, and disadvantages.

### A. SUBSTRATE MATERIAL

A choice of substrate material is very important while designing an antenna. Several substrates are available for designing an antenna. A substrate with low loss tangent ($\delta$), low relative permittivity ($\epsilon_r$) and high thickness is desirable to enhance the performance of an antenna. If loss tangent ($\delta$) increases then dielectric losses also increases which in turn decreases the gain and efficiency of an antenna. Hence, it becomes very important to choose a low loss tangent substrate while designing an antenna. Similarly in the case of the relative permittivity ($\epsilon_r$), if it decreases then the length and width of an antenna increases for required resonance frequency which in turn increases the fringing field and aperture area. Which gives us enhanced bandwidth and gain of an antenna. Moreover, if the relative permittivity of the substrate is high then the magnitude of the electric field reduces considerably within the volume of the substrate and it reduces the gain of an antenna. So, for a required resonant frequency with high gain and bandwidth substrate with low relative permittivity should be chosen. In the case of more thicker substrate fringing field increases which improves the bandwidth and provides more mechanical strength to an antenna. In the literature, the most commonly used substrate for designing AVA antenna are Flame Retardant 4 (FR-4) [45], Rogers RO4003 [10], and Rogers RT/Duroid 5880 [48]. These materials can be employed as per the required parameters and suitability for the antenna.

The detailed comparison of AVA design for different substrate materials is summarized in table 1. They are compared based on the relative permittivity ($\epsilon_r$), loss tangent ($\delta$), the height of substrate(h) in mm, Size of an antenna in ($mm^2$), return loss (S11) in dB, gain in dB, operating frequency range in GHz and applications. It shows that AVA in [49] which is designed by using the RO3006 substrate is most compact with good return loss. But, enhanced gain, wide bandwidth, compact and best return loss is provided by AVA designed by using RO4003 [10]. Hence, the RO4003 substrate with 3.38 permittivity and 0.0027 loss tangent is the best choice for AVA design. The comparison of FR4 and RO3006 is demonstrated in figure 5 [49]. Figure 5(a) is the typical top view of AVA on the FR4 substrate and 5(b) is the top view of AVA on the RO3006 substrate. Both figures show that the RO3006 substrate reduces the size of an antenna. Also, Figure 5(c) and (d) gives a comparison of return losses of FR4 and RO3006 which clearly shows that RO3006 provides better return loss.

### B. SHAPE OF FLARE

The shape of the AVA flare decides the aperture area of an antenna. As the area of flare increases, the radiation will be more which will boost the gain of an antenna. But, further,

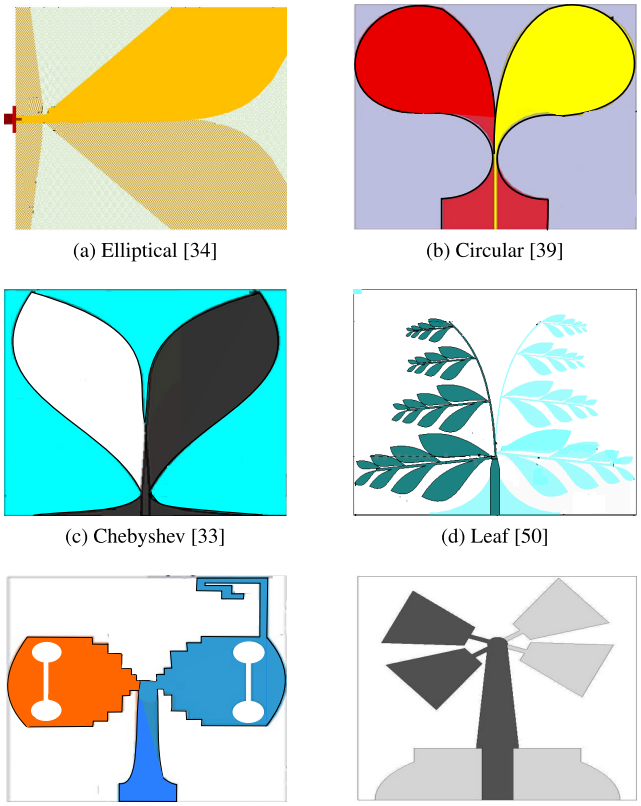

(a) Elliptical [34] (b) Circular [39]

(c) Chebyshev [33] (d) Leaf [50]

(e) Bow Tie [16] (f) Windmill [20]

**FIGURE 6.** Different shapes of flares.

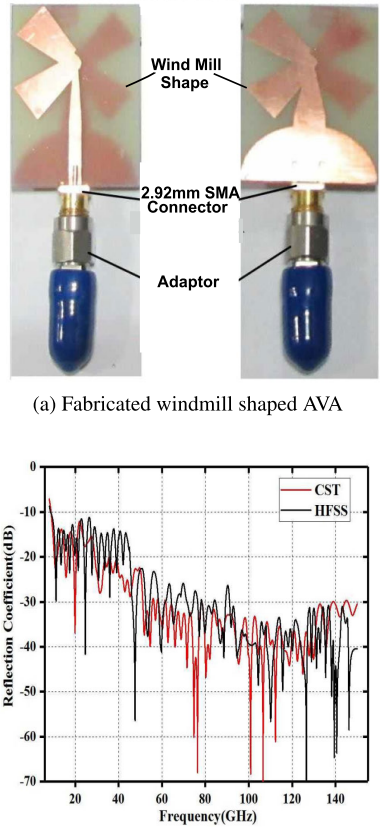


(a) Fabricated windmill shaped AVA

(b) Simulated return loss

**FIGURE 7.** Results of windmill shaped AVA [20].

it will increase the AVA size. The narrow flare size provides a compact antenna but with degraded antenna performance in terms of an antenna gain. Researchers have proposed various antipodal Vivaldi antenna shapes in the literature like elliptical, circular, Chebyshev, leaf structures, etc. The most common flare structure is elliptical shape [34] because of its easy design and implementation as shown in figure 6(a). The elliptical shape can be narrow or wide depending on the rate of increase of edge of AVA flare. The straight-line present in between two endpoints of elliptical shape if extended it will be modified to a circular shape as shown in figure 6(b). This circular shape AVA provides the same radiation pattern in both E and H plane and improves impedance matching [51]. Further, it improves impedance bandwidth to 25:1 as reported in [39]. Also, to improve the range of operating frequency, the researcher has used Chebyshev tapering [33] as it provides good impedance matching at a lower frequency with a stable radiation pattern over almost all frequency range. The leaf structure of AVA is employed to alleviate the cross-polarization of AVA [35], [50]. Although due to this leaf structure the design of an antenna becomes complex as shown in figure 6(d), the design can be made simple and compact by using bow tie [16] and windmill [20] as shown in figure 6(e) and 6(f). But, both bow tie and windmill shapes reduce the AVA gain.

All the different shapes of the flare are shown in figure 6 and the comparison of different shapes of AVA flare is listed in table 2. Figure 6 shows that elliptical shape is easy to implement but it results in more antenna size as per table 2. Leaf structure provides good gain but, its design is complex. Out of these shapes, windmill shape is a suitable shape that provides compact, improved return loss and wideband AVA. Figure 7(a) shows a typical fabricated AVA antenna of windmill shape and its simulated return loss is demonstrated in figure 7(b) which indicates that windmill flare shape outputs compact and wideband antenna [20].

### C. SLOTS

The AVA with slots consists of one or metal parts removed from the flares. Slots play a vital role in the bandwidth enhancement of an antenna. It minimizes the lower cutoff frequency, reduces the sidelobe levels as well as increases the main lobe level [55], [56]. The circular shape of flare with slots increases bandwidth and low-frequency performance of AVA [39], [53]. Circular slots are used to reduce the Radar Cross Section (RCS) in [38]. A compact AVA with reduced co polarization and cross-polarization can be designed by using double tapered slots [50], [52]. Periodic slots with lens enhance the overall performance of AVA. It increases gain, bandwidth, directivity, front to back ratio and reduces sidelobes and dimensions of AVA [57]. Slots with variable capacitors or split-ring resonators are used to design re-configurable AVA for rejecting unwanted bands in [58], [59]. Dual-band

**TABLE 2.** Comparison of antipodal Vivaldi antennas with different flare structures.

| Reference | Flare Shape | Substrate | Size ($mm^3$) | Return Loss (dB) | Gain (dB) | Frequency (GHz) | Application |
|---|---|---|---|---|---|---|---|
| [34] | Elliptical | FR-4 | 100 x 172.14 x 1.6 | -40 | -1-6 | 1-6 | Broad Band |
| [39] | Circular | RT5880 | 64 x 64 x 2.54 | -30 | 3-12 | 4-50 | UWB, 5G |
| [33] | Chebyshev | FR-4 | 100 x 100 x 1.6 | -52 | 4.5-6.8 | 1-35 | UWB, 5G |
| [50] | Leaf | FR-4 | 50.8 x 62 x 0.8 | -35 | 10 | 1.3-20 | UWB |
| [16] | Bow Tie | FR-4 | 26 x 31 x 1.6 | -31 | 0-4.2 | 2.8-3.4<br>4.2-5.1<br>6.1-11.6 | UWB |
| [20] | Wind Mill | FR-4 | 25.5 x 35 x 1.52 | -70 | 4-8.5 | 10-160 | 5G, Ka Band |

**TABLE 3.** Comparison of antipodal Vivaldi antennas with different slots structures.

| Reference | Substrate | Size ($mm^3$) | Return Loss (dB) | Gain (dB) | Frequency (GHz) | Application |
|---|---|---|---|---|---|---|
| [50] | FR-4 | 42 x 36 x 1.6 | -25 | 1.8-6.9 | 3.7-18 | UWB |
| [52] | FR-4 | 60 x 48 x 1 | -40 | 3.7-10 | 2.4-14 | UWB |
| [38] | FR-4 | 32 x 35 x 1.6 | -37 | 4-5.5 | 3-12 | UWB |
| [39] | RT 5880 | 64 x 64 x 0.25 | -30 | 3-12 | 4-50 | UWB,5G |
| [54] | RO 4003 | 101 x 50 x 1.5 | -37 | 8.7-11.5 | 6-18 | UWB |
| [21] | RO 4003 | 40 x 90 x 0.508 | -45 | 6-15 | 3.4-40 | Construction |

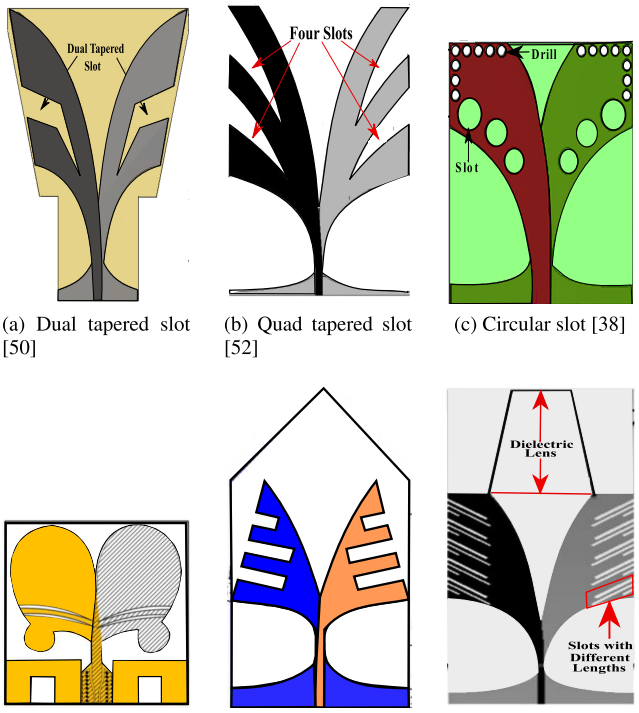


(a) Dual tapered slot [50]
(b) Quad tapered slot [52]
(c) Circular slot [38]
(d) Slots in circular AVA [53]
(e) Slots in balanced AVA [54]
(f) Multiple slots with lens [21]

**FIGURE 8.** AVA design with slots.

AVA by using two wide rectangular slots is given in [60]. Slots with substrate elongation are used to increase end-fire radiation characteristics of balanced AVA [54].

Different AVA with slots as shown in figure 8 and their comparison is given in table 3. In [21], AVA is designed with multiple periodic slots at different locations, different widths and different lengths that provide compact, improved return loss and wide bandwidth as compared to other AVA with slots. AVA with circular slots designed in [38] is very compact but, its gain is less. Therefore, AVA structure designed in [21] can be considered as an appropriate structure within AVA with slots found in the literature for typical AVA antenna. The design of typical rectangular slots with a trapezoidal-shaped dielectric lens is shown in figure 9(a) [10]. In this, antenna 0 is the conventional antipodal Vivaldi antenna (CAVA) with no slots and antenna 1 to 3 are with slots named as periodic slit edge AVA (PSEAVA). Antenna 1 is implemented with five slots of width $W_1$ and length $L_1$. Antenna 2 is implemented with slots given in antenna 1 and five more slots of width $W_2$ and length $L_2$. Antenna 3 is designed as an extension of antenna 2 containing five more slots of width $W_3$ and length $L_3$. The effect of slots on AVA bandwidth and return loss is shown in figure 9(b) for typical rectangular slots with a trapezoidal-shaped dielectric lens [10] where it can be clearly seen that antenna 3 shows the improvement in bandwidth and return loss.

### D. CORRUGATION

Corrugation means repetitive, evenly spaced and same shaped slots made on the outer edge of flares which coincides with an edge of the substrate. The corrugation on flares improves gain and return loss of the AVA. Comb shaped corrugation on elliptical flare is implemented in [23] to efficiently find voids in the concrete beam. Rectangular corrugation along with the elliptical-shaped patch in between two flares improves directivity and reduces sidelobes [40]. Sine wave

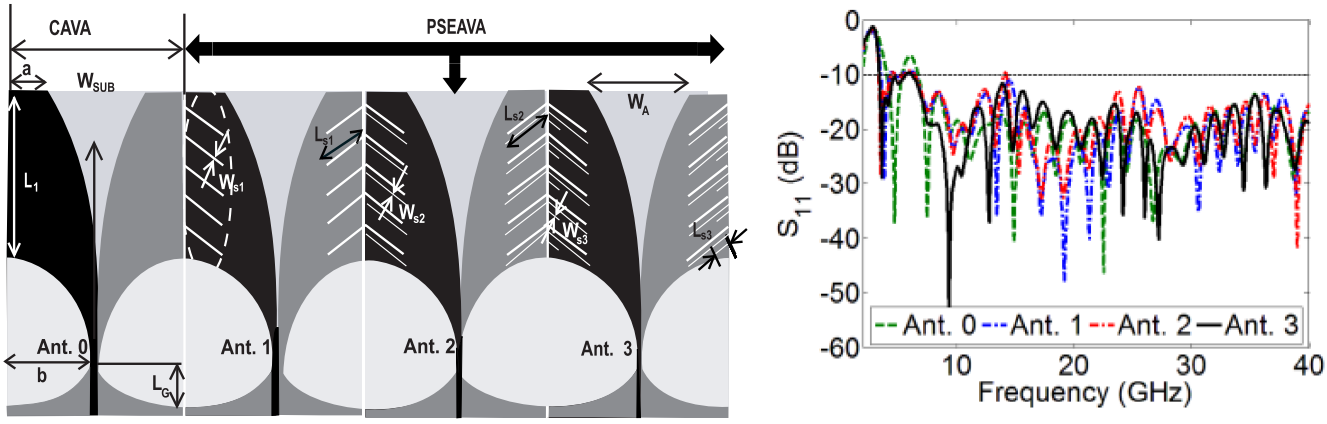


(a) AVA with different slots

(b) Simulated return loss

**FIGURE 9.** Effect of slots on AVA bandwidth and return loss [10].

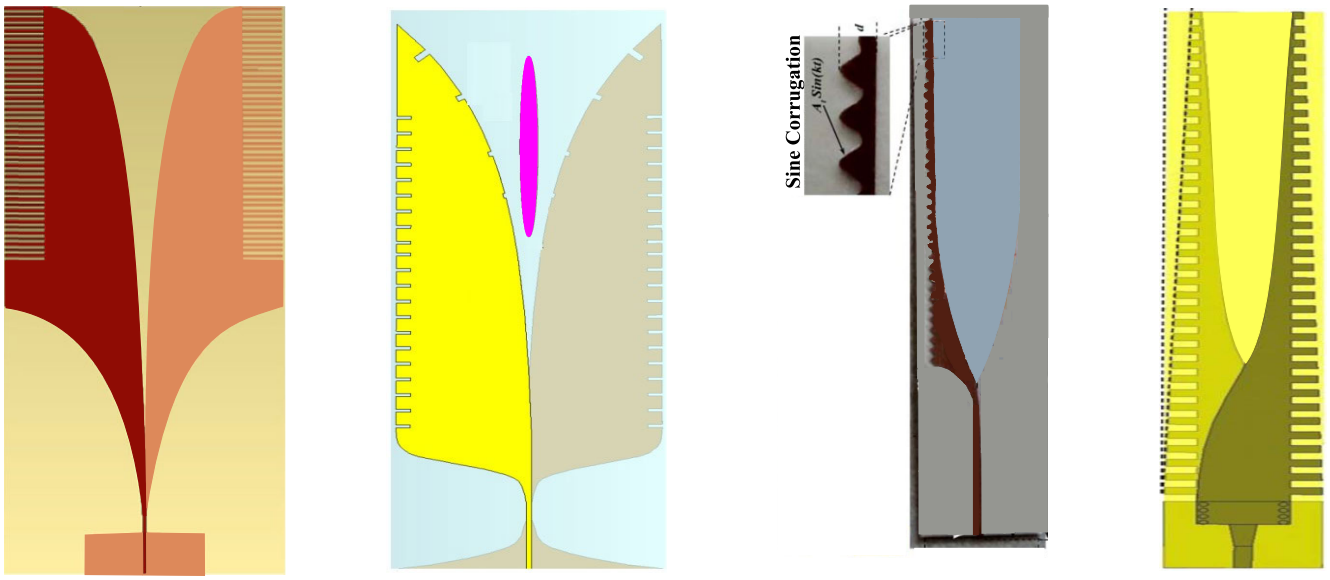


(a) Comb [23]

(b) Rectangular [40]

(c) Sine [61]

(d) Rectangular with different size [62]

**FIGURE 10.** Different shapes of flare corrugation of AVA.

corrugation gives a very large and almost constant gain of above 18dB [61], [63]. It also improves return loss to a great extent. Sine corrugation provides −15dB as a maximum value of return loss over a required bandwidth. The effect of the size of corrugation is demonstrated in [62]. The shape of the corrugation is rectangular. Three types of corrugations discussed in [62] are the same size (design A), decreasing size from start to end (design B) and increasing size from start to end (design C) of the substrate. Design B is shown in figure 10(d). Out of these, a corrugation with decreasing size (design A) gives the best return loss [62], [64]. The same size and decreasing size (design A and B) provides higher gain. But, corrugation with increasing size (design c) reduces return loss and gain. Hence, the same size and decreasing size corrugation types can be used to further improve the AVA parameters.

Different corrugation designs are given in figure 10 and table 4 summarizes AVA with corrugation design comparison. From table 4, we can see that sine shaped corrugation implemented in [61] improves AVA parameters more effectively as compared to other shapes of corrugation. It alleviates AVA size and return loss and enhances AVA gain. Moreover, rectangular corrugation with decreased size provides the constant and highest gain of 20 dB [62]. Figure 11(a) shows a typical fabricated CSAVA-B (Comb Shaped Antipodal Vivaldi Antenna with Bend) antenna [23] and the effect of corrugation on bandwidth, gain, and front to back ratio is shown in figure 11(b,c,d). In this, CAVA means conventional AVA, CAVA-B means conventional AVA with the bend, and CSAVA-B means comb-shaped AVA-B. Figure 11(b) indicates a lower cutoff frequency is 1.7 GHz for CSAVA-B which is lower than CAVA and CAVA-B. Also,

**TABLE 4.** Comparison of antipodal Vivaldi antennas with different corrugation structures.

| Reference | Corrugation Shape | Substrate | Size ($mm^3$) | Return Loss (dB) | Gain (dB) | Frequency (GHz) | Application |
|---|---|---|---|---|---|---|---|
| [23] | Comb | RO 4003 | 120 x 202 x 0.508 | -46 | 7-15 | 1.65-18 | Concrete Beam |
| [40] | Rectangular | RT 6002 | 186 x 77 x 1 | Not Given | 4-16 | 2.5-57 | 5G, UWB |
| [61] | Sine | RT 6002 | 35 x 13 x 1 | -40 | 18-19 | 55-65 | Ka Band |
| [63] | Triangular | RT 6002 | 83.5 x 10.25 x 0.508 | -40 | 11-20 | 26-40 | Ka Band |
| [62] | Rectangular | RT 5880 | 70 x 16 x 0.258 | -30 | 20 | 58-66 | Radar |

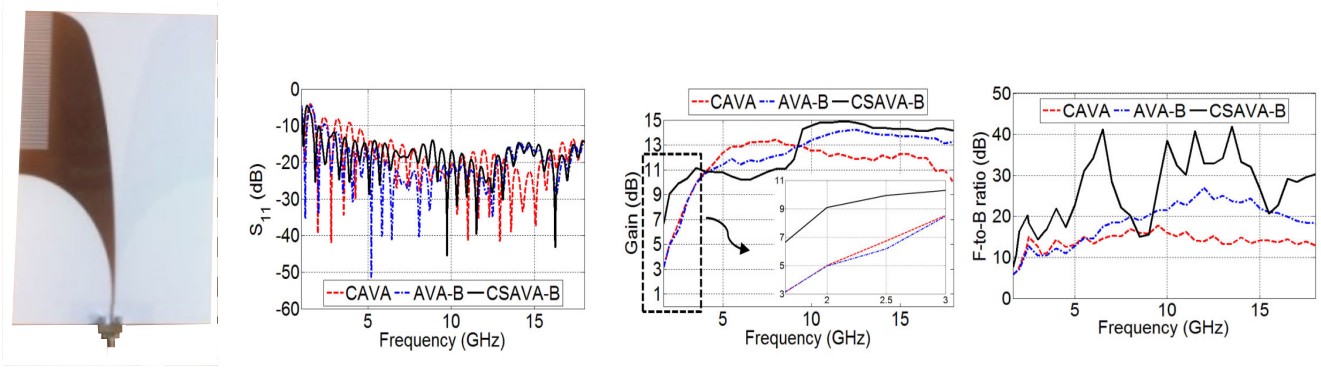


(a) Fabricated CSAVA-B (b) Simulated return loss (c) Simulated gain (d) Simulated front to back ratio

**FIGURE 11.** Effect of corrugation [23].

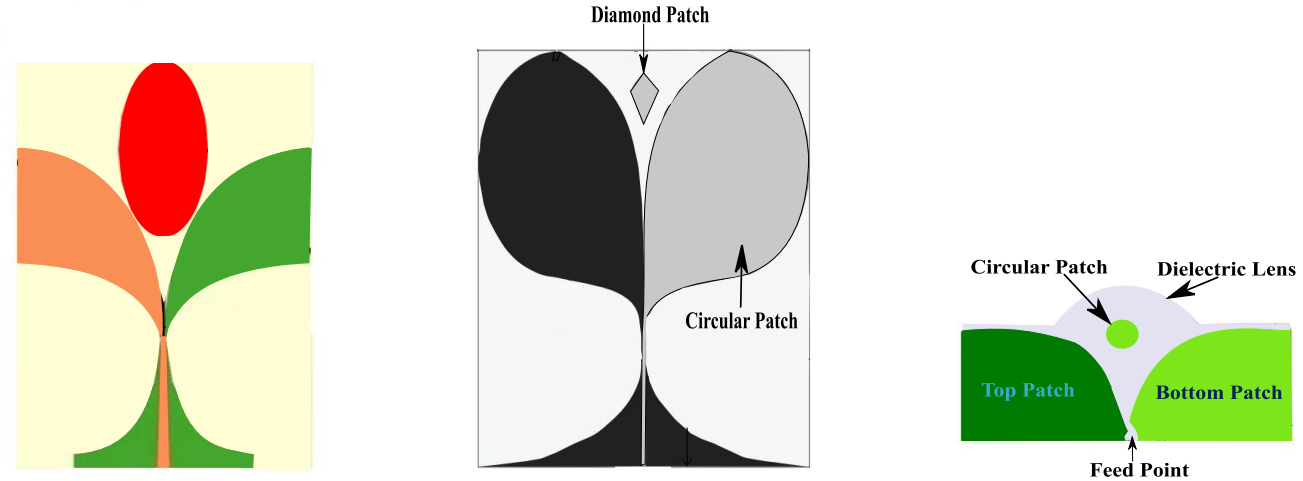


(a) Elliptical patch [42] (b) Diamond patch [65] (c) Circular patch [17]

**FIGURE 12.** Parasitic patch shapes.

figure 11(c) and (d) shows that gain and front to back ratio is higher in CSAVA-B as compared to CAVA and CAVA-B.

### *E. PARASITIC PATCH IN AVA*

The parasitic patch is designed in between two flares of AVA. This parasitic patch couples with main radiating flares to focus radiation beam in the end-fire direction. This maximizes the directivity and hence the gain of AVA [42]. The parasitic patch can be of different shapes like ellipse, diamond, circular, etc. as shown in figure 12. The trapezoidal parasitic patch is designed in [66] to radiate a maximum portion of the beam in the end-fire direction by coupling with the main radiating patch. The dielectric lens with a circular parasitic patch gives a compact and high gain antenna [17]. Elongated parasitic patch with corrugation and band-pass can be implemented in AVA to control beam width and sub-harmonic suppression [67].

The performance comparison of AVA design for different parasitic patch structures is listed in table 5. In [17], the circular parasitic patch with a dielectric lens is implemented in AVA to make it compact for the UWB application. Elliptical patch enhances gain and provides wider bandwidth at the expense of increased AVA size [42]. Figure 13(a) is the typical fabricated AVA with an elliptical parasitic patch

**TABLE 5.** Comparison of antipodal Vivaldi antennas with different parasitic patch structures.

| Reference | Patch Shape | Substrate | Size ($mm^3$) | Return Loss (dB) | Gain (dB) | Frequency (GHz) | Application |
|---|---|---|---|---|---|---|---|
| [42] | Elliptical | RT 6002 | 140 x 66 x 1.5 | -27 | 0-12 | 7-32 | UWB,5G |
| [66] | Trapezoidal | TLC-30 | 124 x 66 x 1.575 | -32 | 3-12 | 6-26.5 | UWB, 5G |
| [17] | Circular | FR-4 | 34 x 16 x 0.8 | -30 | 3.27-6.7 | 3.01-10.6 | UWB |
| [65] | Diamond | Teflon F4B | 124 x 116 x 0.5 | -50 | 2.5-9.8 | 2.2-12 | UWB |
| [67] | Elliptical | RT 5880 | 33.8 x 16 x 0.25 | -30 | 6.35-8.51 | 27-31 | 5G |

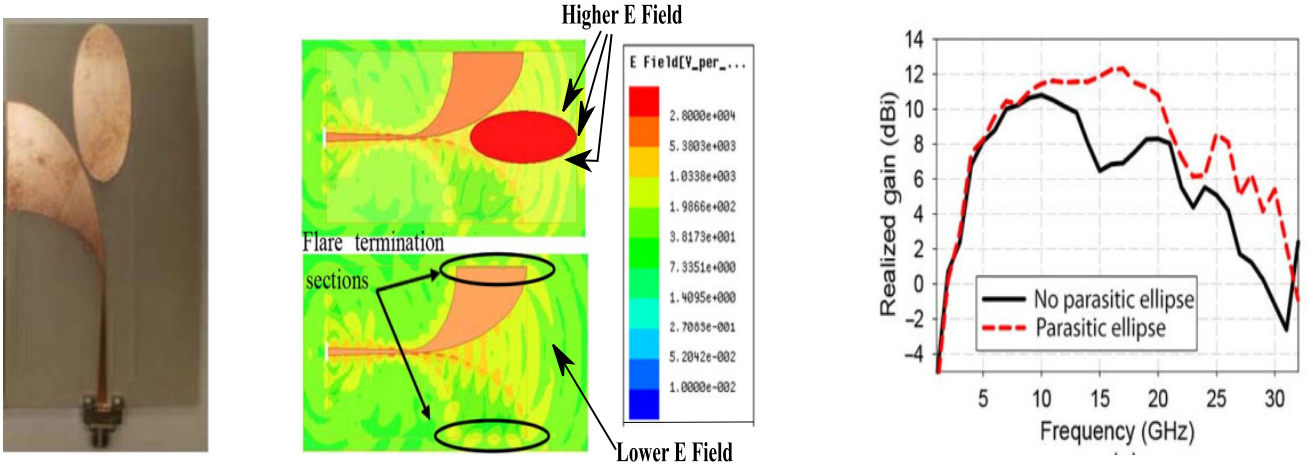


(a) Fabricated AVA with elliptical patch

(b) Simulated electric field

(c) Simulated gain

**FIGURE 13.** Effect of parasitic patch [42].

[42]. As the size of the parasitic patch is more, the size of AVA with a parasitic patch is more as compared to conventional AVA. But, this parasitic patch increases radiation in the end-fire direction as shown in figure 13(b). As the more electric field is generated, gain also increases as shown in figure 13(c).

### *F. DIELECTRIC LENS*

The dielectric lens is also called as director. It is placed in between two flares of AVA at the end of the aperture. The dielectric lens should have higher permittivity, it should work as a waveguide to direct most of the energy towards the aperture center and its phase velocity should be low [68]. As radiation is directed in one direction, the gain of antenna increases [15], [69]. It also improves the symmetry of the radiation pattern [70]. The different shapes of the lens are diamond [68], elliptical [18], rod shape [75], trapezoidal [71], [76] etc. The rod-shaped dielectric lens has low insertion loss and high mutual decoupling efficiency. Also, it provides a frequency-independent radiation pattern. The titled beam at higher frequency can be corrected by using dielectric lens [18]. Dielectric lens and slots are used to enhance gain, bandwidth and the front to back ratio of AVA [72]. To achieve a higher gain multilayer dielectric lens with different permittivity at different layers is implemented in [22]. As compared to the circular shape dielectric lens, the trapezoidal shape dielectric lens increases the gain of an antenna [10], [72], [77]. By enclosing AVA and its dielectric lens by another dielectric, low cross-polarization, high front to back ratio, large gain, wide bandwidth and correction of beam tilting can be achieved [7]. By using the dielectric lens with other performance enhancement methods like an array, slots, corrugation, etc. improves the parameters of AVA very effectively [73], [74].

Different dielectric lens designs are given in figure 14 and AVA with dielectric lens design comparison is given in table 6. The highest and constant gain of 18-20 dB and wide bandwidth of 5-50 GHz is obtained in [7] which used a trapezoidal-shaped dielectric lens. Further, the highest return loss of $-52$dB is achieved in [74] and [22] by using a circular-shaped dielectric lens. Figure 15(a) is the typical fabricated AVA with a multi-layer planar dielectric lens (AVA-MPDL) [22]. These three layers are of different permittivity. Outer layer permittivity is the same as that of the substrate. Figure 15(b) shows that conventional AVA suffers from beam tilting at higher frequencies which are effectively reduced with the help of a dielectric lens. A noticeable gain enhancement is achieved as shown in figure 15(c). It also improves front to back ratio as depicted in figure 15(d).

**TABLE 6.** Comparison of antipodal Vivaldi antennas with different dielectric structures.

| Reference | Substrate | Size ($mm^3$) | Return Loss (dB) | Gain (dB) | Frequency (GHz) | Application |
|---|---|---|---|---|---|---|
| [68] | RT6002 | 78 x 44 x 9.2 | -40 | Not Given | 2.2-12 | Breast Cancer Detection |
| [15] | RO4003C | 30 x 55 x 0.508 | -50 | 10-13 | 5-50 | mWave Imaging |
| [69] | FR-4 | 76 x 130 x 1 | -36 | 2-7 | 3.1-14 | UWB |
| [70] | RT 5880 | 105 x 56 x 1.5 | Not Given | 9.41-12.09 | 6-20 | UWB |
| [71] | RO4003 | 60 x 40 x 1 | -45 | 2-16.5 | 3.68-50 | UWB |
| [18] | AD255 | 96 x 50 x 3.15 | -27 | 5-14.7 | 3-18 | UWB |
| [72] | RO4003 | 96 x 100 x 0.508 | -40 | 2-12 | 1-30 | Concrete Construction |
| [22] | RT 5880 | 171.8 x 149.8 x 1 | -52 | 1-16.5 | 1.3-30 | UWB |
| [7] | RO4003 | 31.6 x 110 x 0.8 | -50 | 18-20 | 5-50 | mmWave |
| [73] | RO4350 | 166 x 70 x 0.762 | -42 | 10.3-14.8 | 4.7-20 | Microwave |
| [74] | RT 5880 | 66.4 x 50 x 1 | -52 | 5-8 | 4-30 | UWB and Radar |

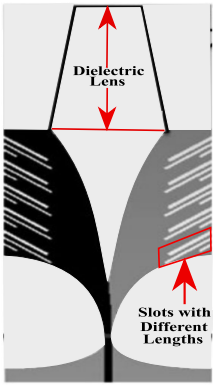


(a) Multiple slots with trapezoidal lens [10]

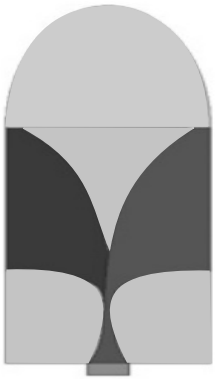

(b) Elliptical [18]

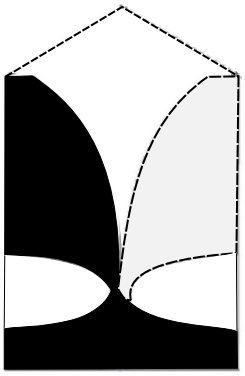

(c) Triangular [70]

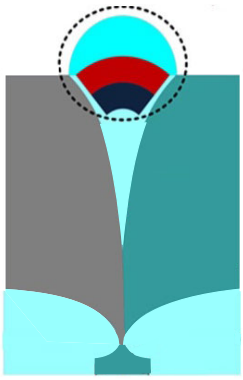

(d) Circular with multi-layer [22]

**FIGURE 14.** Different shapes of dielectric lens of AVA.

### G. BALANCED ANTIPODAL VIVALDI ANTENNA (BAVA)

The structure of Balanced Antipodal Vivaldi Antenna (BAVA) is shown in figure 16. It consists of three copper layers. Outer two copper layers act as ground layers and the middle layer acts as a conductor. All copper layers are separated by substrates. As explained in figure 17, this structure balances the loading of dielectric material in between conductor and ground plane. Due to this balancing beam squint is greatly reduced [68]. Beam squint means a change in beam direction due to frequency, polarization or orientation. Substrate elongation in BAVA and slots on its flare enhances end-fire performance and provides higher front to back ratio [54]. BAVA with transformation optics is used in [14] to improve the gain, sidelobe level, and cross-polarization. Antenna gain and beam tilting can be improved by using BAVA and patch in between two flares of BAVA [36]. A noticeable reduction in beam squint can be achieved by eliminating substrate in between two metal flares [11]. Wideband BAVA can be changed to notch band BAVA by including a quarter wavelength spur line in feeding microstrip line [78].

Table 7 lists the performance comparison of BAVA design. BAVA with improved return loss and bandwidth is implemented in [36]. Moreover, a compact BAVA is implemented in [11] by introducing corrugation in it. Figure 18(a) is the top view and 18(b) is the bottom view of the typical fabricated BAVA. This BAVA is designed by using corrugation, slots and by removing substrate present in between two flares. Figure 18(c) shows that the modified BAVA minimizes beam squint. In this research, four types of BAVA are conventional BAVA, BAVA with symmetric substrate cut-out (BAVA-SC), BAVA with asymmetric cut-out (BAVA-AC) and BAVA- AC with dual-scale slotted edges (BAVA-AC-DSE). The BAVA-AC-DSE alleviates sidelobe levels effectively as shown in figure 18(d).

### H. METAMATERIAL

The metamaterial is designed with the help of two materials. Unit cell defines different types of metamaterials, for example, epsilon negative, mu negative, double negative, chiral, isotropic, anisotropic, etc. [82]. The AVA with and without metamaterial is given in figure 19. It shows that in between two flares of AVA, metamaterial design is implemented. In [31], 1 × 8 antipodal Vivaldi antenna array is implemented with an anisotropic metasurface (MS) and

**TABLE 7.** Comparison of balanced antipodal Vivaldi antennas.

| Reference | Substrate | Size ($mm^3$) | Return Loss (dB) | Gain (dB) | Frequency (GHz) | Application |
|---|---|---|---|---|---|---|
| [54] | RO4003 | 101 x 50 x 1.5 | -37 | 8.7-11.5 | 6-18 | UWB |
| [14] | RT 6002 | 74 x 44 x 0.508 | -30 | 7.8-10.8 | 8-16 | UWB |
| [36] | RT5880 | 110 x 44 x 3 | -58 | 1-16 | 2-40 | UWB,5G |
| [11] | RT 5880 | 79.9 x 24 x 0.508 | -27 | 10.2-14.5 | 10-40 | UWB |
| [78] | RO 5880 | 162 x 140 x 3.15 | -30 | 3-10 | 0.92-9.7 | UWB |

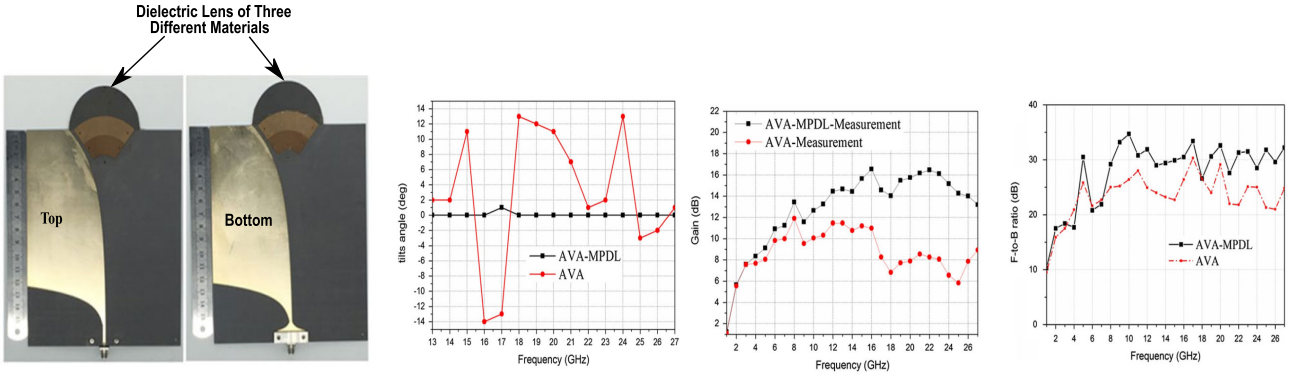


(a) Fabricated AVA with dielectric lens (b) Simulated E plane beam tilt (c) Simulated Gain (d) Simulated front to back ratio

**FIGURE 15.** Effect of dielectric lens [22].

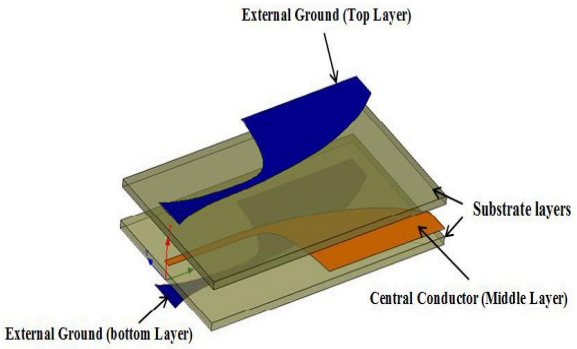


**FIGURE 16.** Structure of balanced antipodal Vivaldi antenna (BAVA) [68].

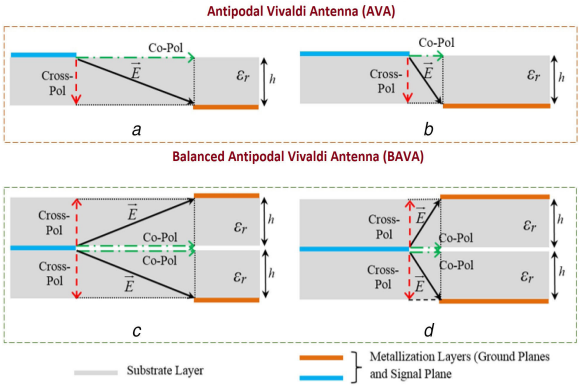


**FIGURE 17.** Schematic representation of co-polarized and cross polarized components of the electric field vector in AVA and BAVA [78].

located at the aperture, resulting in low cut off frequency. Modified W shaped metamaterial unit cells are implemented in [30]. In this, the gain is increased by including slots into the flare with an irregular spacing distance between each other. Metamaterial unit cells are printed on both sides of an antenna. Index near-zero metasurface is implemented in [46] to increase the gain and bandwidth. A defected ground slots are added on both edges of an antenna to minimize the lower frequency. Zero index metamaterial by using non-uniform zig-zag structures is implemented above the aperture area of the antipodal Vivaldi antenna in [5] which provides good radiation pattern, low sidelobes, and narrow beamwidth. In [9], gain enhancement of a millimeter-wave AVA by Epsilon-Near-Zero metamaterial is proposed. In this H shaped metamaterial unit cells are implemented on the triangular shape which is above the aperture area of AVA. A negative index metamaterial (NIM) is implemented in [79] for UWB application. NIM is designed by using square spiral unit cells that are inserted at the right angle on AVA at the center. Snug-in negative-index metamaterial is implemented in [28] for the performance-boosting of AVA. In these seven layers of metamaterial surfaces are implemented and inserted at the right angle on AVA in the center of the end to enhance the gain. Zero Index Metamaterial (ZIM) is also used to gain enhancement [80]. AVA signal radiation in unwanted direction can be avoided and hence gain can be enhanced to a larger extent by using metamaterial slabs around AVA [81].

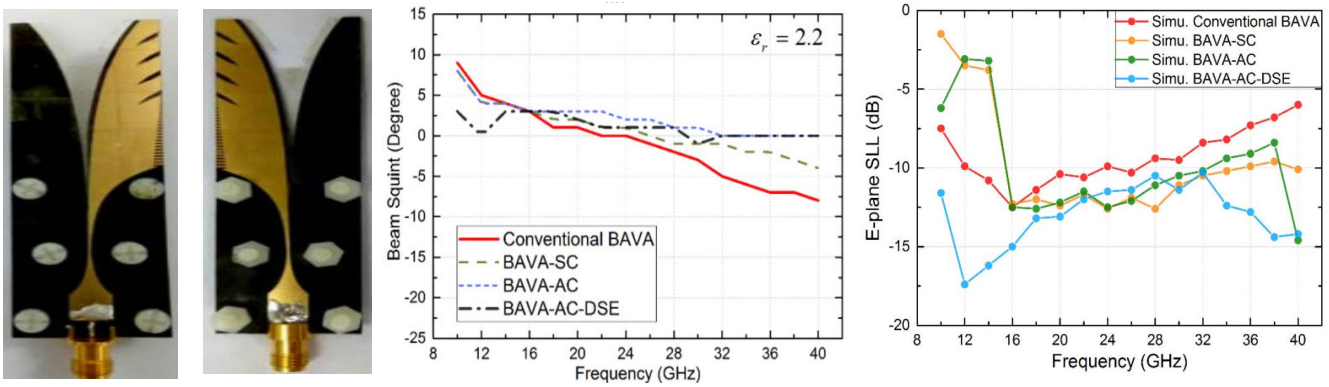


(a) Fabricated BAVA-AC-DSE top view (b) Fabricated BAVA-AC-DSE bottom view (c) Simulated E Plane beam squints (d) Simulated sidelobe level(SLL)

**FIGURE 18.** Effect of balanced AVA [11].

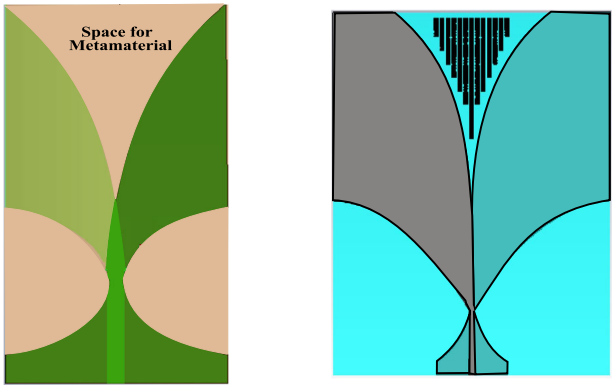


(a) AVA without metamaterial (b) AVA with metamaterial [5]

**FIGURE 19.** AVA with and without metamaterial.

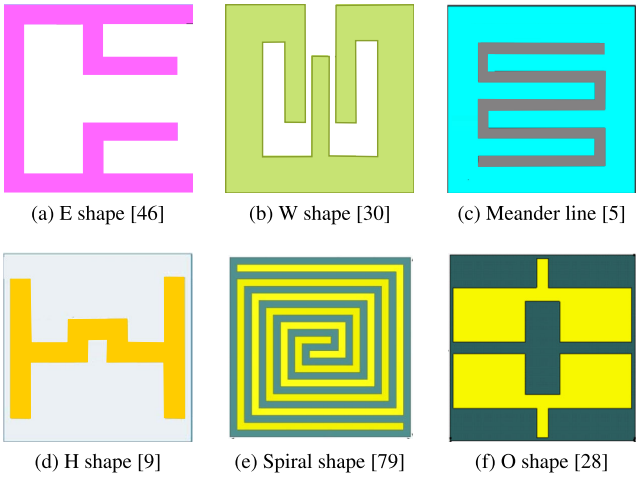

(a) E shape [46] (b) W shape [30] (c) Meander line [5] (d) H shape [9] (e) Spiral shape [79] (f) O shape [28]

**FIGURE 20.** Different metamaterial unit cells.

Different metamaterial Unit Cell (MUC) designs are given in figure 20 and an overview of AVA with metamaterial design comparison is presented in table 8. Enhanced gain, compact, improved return loss and wider bandwidth are implemented in [9] by using modified H shaped metamaterial on the dielectric lens. Further, the smallest size AVA with modified I shaped metamaterial is implemented in [80]. From all these comparisons, we can say that deciding the shape and position of metamaterial is the daunting task. Figure 21(a) is the typical fabricated AVA with epsilon near zero(ENZ) metamaterial [9]. Modified H shaped metamaterial is present on a triangular-shaped dielectric lens. Metamaterial enhances return loss as shown in figure 21(b). As shown in figure 21(c), metamaterial provides higher and nearly constant gain as compared to conventional AVA.

### *I. AVA ARRAY*

The primary concern of the AVA array is to increase its gain. Single AVA antenna performance increases effectively by implementing AVA array. But, care should be taken at the time of designing its feeding network to match the input impedance. Array structure provides high gain but, side lobes are more and mutual coupling among array elements gets introduced [29]. By reducing the distance between array elements, sidelobe levels can be reduced at the cost of the increase in mutual coupling. Thus it is required to apply different methods of mutual coupling reduction methods. Corrugation and triangular metal directors are used with AVA array in [19], [44] to achieve high and constant gain, low sidelobes and reduction in beam squint. Balanced Antipodal Vivaldi Antenna (BAVA) array not only gives wide bandwidth but also enhances other parameters of BAVA [83]. AVA mechanical robustness can be increased by implementing AVA planer structure [84], [85]. Also, the planar structure enhances the gain and bandwidth of AVA. AVA array with the rod-shaped dielectric lens has low insertion loss and high mutual decoupling efficiency. Further, it provides a frequency-independent radiation pattern [75]. AVA array with substrate integrated waveguide (SIW), corrugation and rectangular dielectric lens are used in [8] to achieve gain higher than 18dB. Substrate Integrated Waveguide (SIW) reduces

**TABLE 8.** Comparison of antipodal Vivaldi antennas with different metamaterial structures.

| Reference | Substrate | Size ($mm^3$) | Return Loss (dB) | Gain (dB) | Frequency (GHz) | Application |
|---|---|---|---|---|---|---|
| [31] | RT5880 | 60 x 28.2 x 0.787 | -30 | 9.35-12 | 24.1-28.5 | 5G |
| [30] | F4B | 55.4 x 30 x 1 | -23 | 11.52 | 8.81-10.22 | UWB |
| [46] | F4BM265 | 130 x 80 x 1 | -27 | 2.27-14 | 1.13-12 | UWB |
| [5] | FR-4 | 140 x 96 x 0.76 | -45 | 9.5-12 | 1.3-12 | UWB |
| [9] | RO 4003 | 40 x 85 x 0.2 | -52 | 14-17.2 | 23-40 | Ka,5G |
| [79] | RT 5880 | 30 x 60 x 0.787 | -27 | 3-8.3 | 4.7-11 | UWB |
| [28] | RT5880 | 100 x 50 x 0.787 | -35 | 7.42-15.4 | 6.5-20 | UWB |
| [80] | Ferro A6S | 22 x 21.7 x 1 | -45 | 12-13.2 | 57-66 | Ka,5G |
| [81] | RO 4003 | 60 x 40 x 0.508 | -40 | 2-17 | 3.68-43.5 | mmWave |

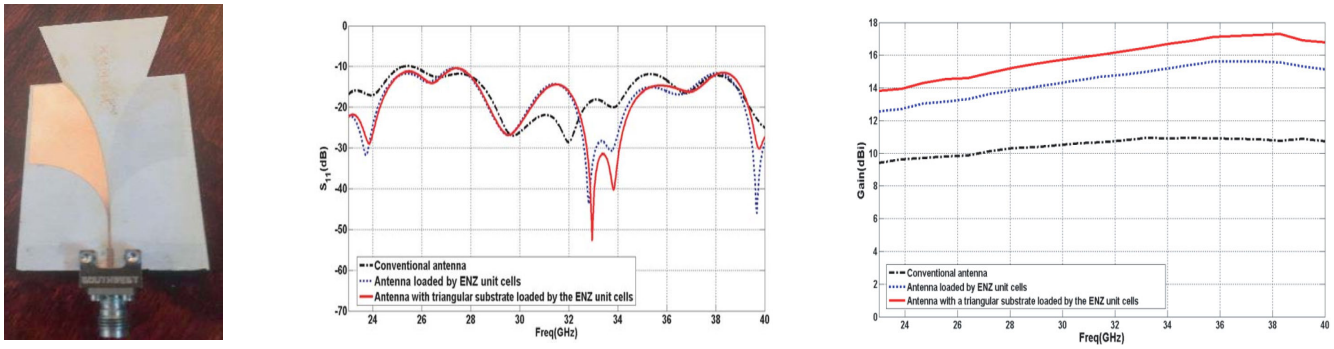


(a) Fabricated AVA with metamaterial

(b) Simulated return loss

(c) Simulated gain

**FIGURE 21.** Effect of metamaterial [9].

**TABLE 9.** Comparison of antipodal Vivaldi antennas arrays.

| Reference | Array Size | Substrate | Size ($mm^3$) | Return Loss (dB) | Gain (dB) | Frequency (GHz) | Application |
|---|---|---|---|---|---|---|---|
| [29] | 1 x 8 | RT 5880 | 28.823 x 60 x 0.787 | -27 | 6.96-11.32 | 24.55-28.5 | 5G |
| [44] | 1 x 8 | RT 5880 | 54.4 x 28.2 x 0.508 | -19 | 12.3-12.9 | 24.75-27.5 | 5G |
| [83] | 1 x 7 | FR-4 | 50 x 190 x 0.64 | -33 | 8-13 | 3-9 | UWB |
| [84] | 7 x 7 | RO 6002 | 266 x 294 x 1.5 | -38 | 12.6-16.5 | 8-12 | UWB |
| [85] | 4 x 4 | RT 5880 | 80 x 80 x 20 | Not Given | Not Given | 2-7.2 | UWB |
| [8] | 1 x 4 | RT 5880 | 78.3 x 43.7 x 0.254 | -23 | 23 | 57-64 | mmWave |

mutual coupling between array elements [86], [87]. AVA Array structure is very useful in medical image processing like breast cancer detection to obtain the exact results [88].

Array feeding can be given in two ways. First by using a single feed and power divider network as shown in figure 22. The second method is to apply separate feeding to each AVA element as shown in figure 23. The performance comparison of AVA array design is given in table 9. It shows that all AVA array designs have improved gain at the cost of increased size. Array performance can be further improved by incorporating other performance enhancement techniques with AVA array. The AVA with the best gain of 23 dB is implemented in [8]. Compact AVA array is implemented in [19].

Figure 24(a) is the typical fabricated 1 × 4 AVA array [8]. Each array element is designed by using corrugation and substrate integrated waveguide (SIW). This SIW structure is a via in the substrate and it is very helpful to reduce mutual coupling among array elements. Figure 24(b) is the simulated and measured results of gain and return loss for a single AVA antenna. Figure 24(c) is the simulated and measured results

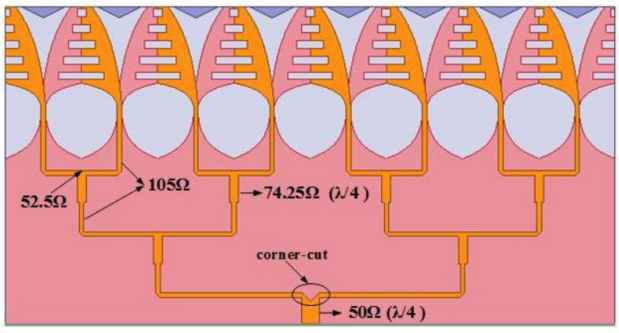


**FIGURE 22.** Antipodal Vivaldi antenna (AVA) array with power divider feeding [44].

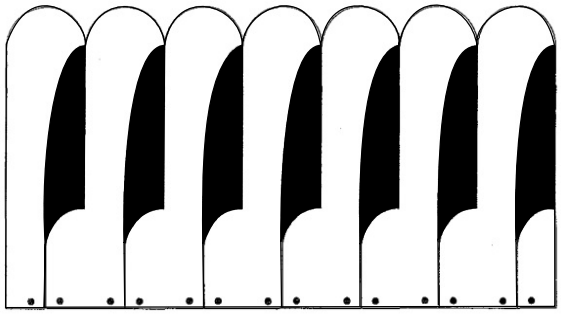

(a) AVA array with separate feeding (Front View) [83]

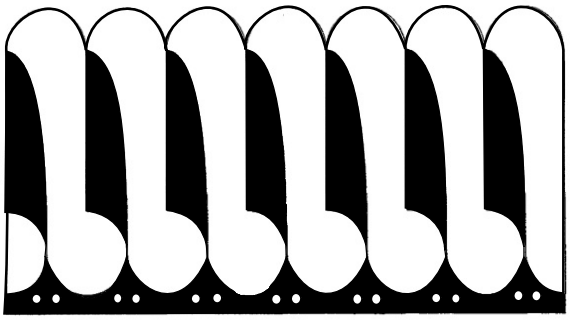

(b) AVA array with separate feeding (Back View) [83]

**FIGURE 23.** AVA Array.

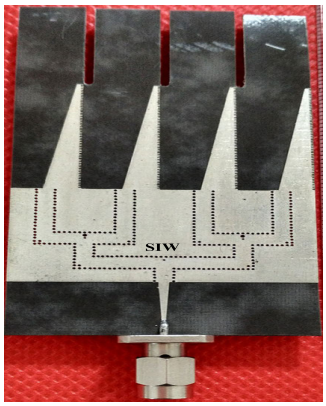


(a) Fabricated AVA array

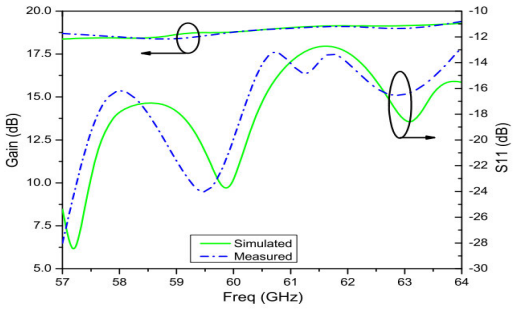


(b) Simulated and measured return loss and gain for single AVA

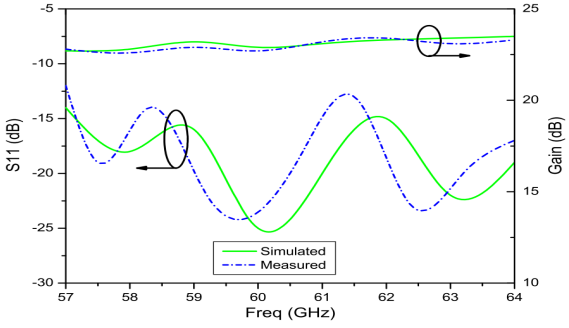


(c) Simulated and measured return loss and gain for AVA array

**FIGURE 24.** Effect of AVA array [8].

of gain and return loss for a 1 × 4 AVA array. Single AVA gives 18.5 dB gain whereas array gives 23 dB gain which is much better than a single antenna. Also, an array structure improves return loss as shown in figure 24(c).

### J. COMPUTATIONAL INTELLIGENCE

The performance parameters of AVA can be enhanced with the help of computational intelligence (CI) techniques like PSO, multi-objective PSO, and multi-objective genetic algorithm (MOGA). As the design of AVA is inherently multi-objective, MOPSO and MOGA are employed by the researchers to obtain optimum trade-offs between two or more below mentioned parameters:

- Beamwidth
- Bandwidth
- Directive
- Dimensions
- Cross polarization
- Reflection coefficient
- Lower cut-off frequency
- Transient distortion
- Sidelobe level (SLL)

In [27], a compact BAVA of size 32 mm × 35 mm × 1.6 mm is designed with the help of a conformal finite difference time domain (CFDTD) method using PSO. The multi-objective PSO (MOPSO) can be used to design the antenna which can meet multiple required objectives. The side-lobe level reduction and optimization of beam-width are achieved in [89]. Also, it can be used to alleviate transient distortion, reflection coefficient, and cross polarization [24]. The main advantage of the CI technique is that we can train it as per the requirement of an application and it is possible to concentrate on required parameters for optimization. Further, the CI technique has disadvantages also like it consumes more time and results may drastically vary if training is not done properly. So, achieving optimum solution may require more iterations which may consume more time as compared to other antenna performance enhancement methods available in the literature.

Table 10 describes the comparison of AVA designs with different CI techniques found in the literature. From this table, it can be seen that PSO is frequently used for antenna parameter optimization. As shown in the table, AVA implemented by using the MOPSO technique gives an improved

**TABLE 10.** Comparison of antipodal Vivaldi antennas with different computational intelligence techniques.

| Reference | CI Technique | Substrate | Size ($mm^3$) | Return Loss (dB) | Gain (dB) | Frequency (GHz) | Application |
|---|---|---|---|---|---|---|---|
| [24] | MOPSO | RF35 | 100 x 100 x 0.76 | -45 | 4.5 - 9 | 2.6 - 11 | UWB |
| [89] | MOPSO | RO4003 | 120 x 120 x 0.813 | -40 | 13.7 - 17.2 | 3 - 11 | UWB |
| [90] | MOGA | FR4 | 300 x 369.31 x 1.6 | -33 | 4-6.8 | 0.39 - 0.8 | Radar |
| [27] | CFDTD-PSO | FR4 | 32 x 35 x 1.6 | -27 | -2.5 - 5.8 | 3.1 - 10.6 | UWB |

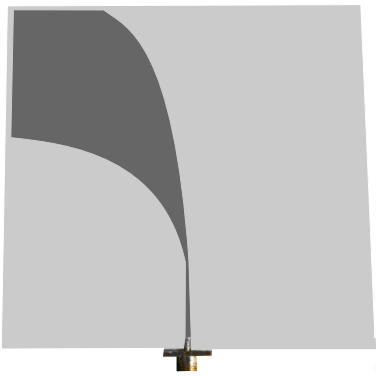

(a) Fabricated AVA

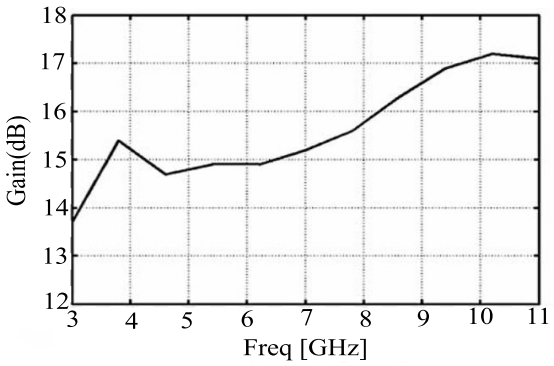


(b) Gain versus frequency graph

**FIGURE 25.** Results of AVA implemented with MOPSO technique [89].

gain in the range of 13.7 dB - 17.2 dB for UWB applications and the same is shown in figure 25(b). Figure 25(a) is the fabricated AVA whose dimensions are optimized by using a multi-objective PSO technique to improve the gain, to reduce side-lobe level, and to optimize beamwidth.

### *K. SUBSTRATE INTEGRATED WAVEGUIDE (SIW)*

Antenna operating at higher frequency bands suffers from higher radiation losses. Therefore, to take the advantages of metallic waveguide many researchers have employed SIW in AVA design to overcome such radiation losses at higher frequencies. It provides the advantages of metallic waveguide antenna like high gain, low losses, high power capacity, and low cross-polarization. The SIW structure consists of metallic vias in the substrate as shown in figure 26 [8]. This structure helps in the direct transmission of electromagnetic waves

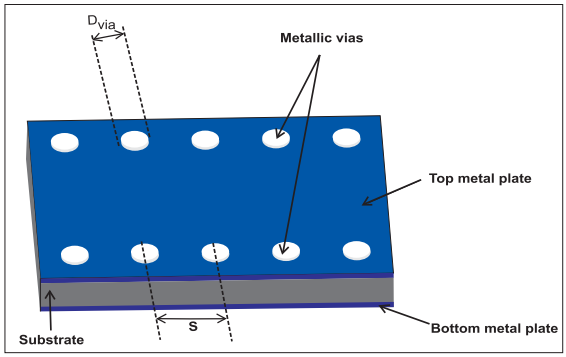


**FIGURE 26.** Structure of SIW [8].

from patch to the ground which in turn reduces the surface wave transmission and hence alleviates the radiation losses. The AVA with SIW is implemented in [19] to enhance the resolution of human burned skin and skin cancer images. The AVA array of four elements with SIW feeding is implemented in [8] to provide a very high gain of 23 dB and a compact size of 78.3 mm $\times$ 43.7 mm $\times$ 0.254 mm. The multi-layer (including air-filled layer) with SIW can be used in AVA array to achieve enhanced gain and low insertion loss [32]. The single AVA with SIW also provides better gain and low insertion loss. Hence, SIW is an appropriate solution where low losses are essential.

Table 11 proves the pivotal role of the SIW technique in the antenna parameter enhancement. From table 11, it can be seen that the SIW can be used to reduce the size of an antenna and to achieve higher gain. Further, its significance in improving isolation is depicted in figure 27. Figure 27(a) is the fabricated AVA array with SIW and figure 27(b) shows improvement in the isolation level of AVA array elements. This mutual coupling is increased by 6 dB after incorporating SIW and dielectric rod as shown in figure 27(b). Table 12 gives the detail of various methods of AVA performance enhancement concerning their trivial points, parameters to be affected, advantages and disadvantages. Table 12 gives a concise review of all AVA parameter enhancement methods which would help the researchers to select the appropriate AVA parameter enhancement technique(s) for their application.

## III. VALIDATION OF PERFORMANCE ENHANCEMENT TECHNIQUES

In this section, we have validated some of the important performance enhancement techniques explained in the previous

**TABLE 11.** Comparison of antipodal Vivaldi antennas with SIW.

| Reference | Array Size | Substrate | Size ($mm^3$) | Return Loss (dB) | Gain (dB) | Frequency (GHz) | Application |
|---|---|---|---|---|---|---|---|
| [19] | 1 x 5 | RT5880 | 20 x 17.5 x 0.254 | -17 | 6.2-8.2 | 58-64 | mmWave |
| [75] | 1 x 8 | RO 4003 | 100 x 90 x 1.524 | -38 | 12.6-16.5 | 8-12 | UWB |
| [86] | 1 x 3 | RO 5880 | 45 x 50 x 0.78 | -27 | 7.1 - 8 | 13 - 17 | Ku band |
| [87] | 1 x 4 | RT5880 | 100 x 20 x 0.508 | -27 | 11.45 - 13.86 | 29 - 36 | 5G |

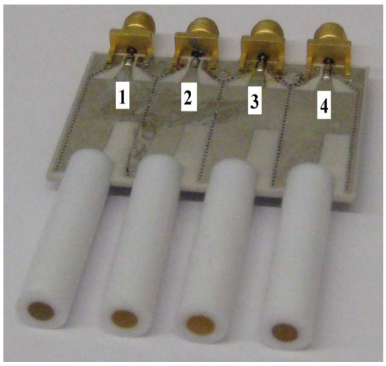


(a) Fabricated AVA

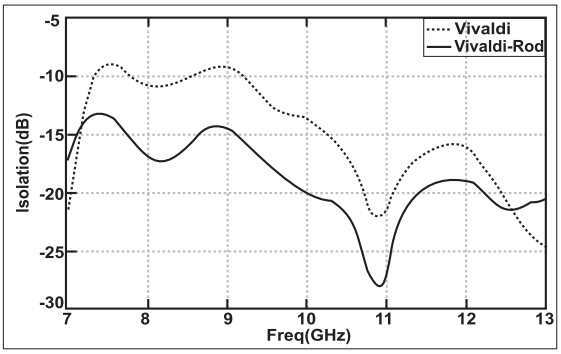


(b) Isolation graph

**FIGURE 27.** Results of AVA implemented with SIW [75].

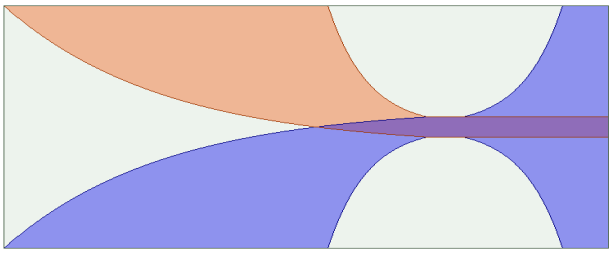

(a) Conventional AVA

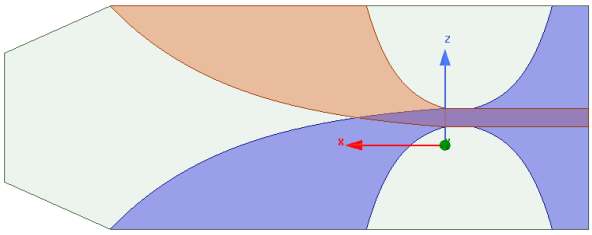

(b) AVA with dielectric lens

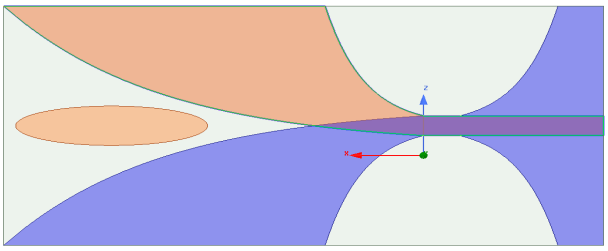

(c) AVA with parasitic patch

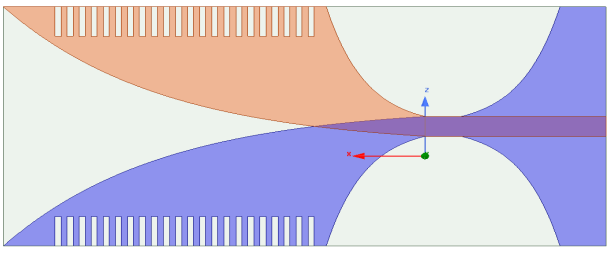

(d) AVA with corrugations

**FIGURE 28.** Design of AVA with different enhancement methods.

section by using a basic conventional AVA design. As it is not possible to design all the AVAs with their performance enhancement methods available in the literature, we have designed a basic conventional AVA with the different substrate, dielectric lens, parasitic patch, and corrugation keeping fixed dimensions, frequency, flare shape, and feeding network. All simulated results are obtained by simulating the designed AVA by using HFSS version 19 software and some parameter enhancement techniques are incorporated in conventional AVA to validate their effect on different parameters of AVA.

Figure 28 shows the design of AVA with different AVA parameter enhancement techniques. Figure 28(a) is the conventional AVA and it is simulated for different substrates like FR4, RO 4003, and RT/ duroid 5880. All other designs are implemented on RT/ Duroid 5880 substrate. Figure 28(b) is the AVA with the trapezoidal dielectric lens, figure 28(c) is AVA with an elliptical parasitic patch, and figure 28(d) is the AVA with rectangular corrugations. We have simulated some of the enhancement techniques to validate their importance in AVA parameter enhancement and which can be further employed to other enhancement

**TABLE 12.** Details of AVA performance enhancement techniques.

| Method | Details of Method | Reference |
|---|---|---|
| Choice of Substrate | **Trivial Point:** Substrate should have low permittivity and low loss tangent<br>**Parameters:** Size, gain, efficiency, bandwidth<br>**Advantages:** Substrate with low permittivity and loss tangent gives high gain, high efficiency and wide bandwidth while substrate with high permittivity improves return loss and reduces antenna size.<br>**Disadvantages:** Substrate with low permittivity and low loss tangent are costly and not easily available. | [49], [91]<br>[92], [93]<br>[94] |
| Flare Structure | **Trivial point:** Flare structure decides aperture area of an antenna for radiation<br>**Parameters:** Input impedance, size, return loss, bandwidth<br>**Advantages:** Circular shape provides good impedance matching, Chebyshev gives stable radiation pattern, bow tie and windmill shape make AVA compact.<br>**Disadvantages:** More aperture area increases AVA size and AVA design becomes complex in leaf structure. | [51], [95]<br>[96], [97]<br>[98] |
| Slots | **Trivial Point:** Slots are helpful for input impedance matching and bandwidth adjustment<br>**Parameters:** Bandwidth, side lobe level, return loss, co polarization and cross polarization<br>**Advantages:** Reduces lower cut-off frequency and hence increases bandwidth, minimizes sidelobe and back lobe level, improves return loss and co polarization<br>**Disadvantages:** Complex antenna design, low efficiency, higher cross-polarization, low front to back ratio, low directivity | [99], [100]<br>[101], [102]<br>[103] |
| Corrugation | **Trivial Point:** It introduces changes in the current path.<br>**Parameters:** Gain, return loss, side lobe level, front to back ratio, bandwidth<br>**Advantages:** Enhanced gain, improved return loss, low side lobe level, increased front to back ratio, wide bandwidth<br>**Disadvantages:** Complex in antenna design and fabrication, reduces input impedance | [23], [40]<br>[62], [104] |
| Parasitic Patch | **Trivial point:** It focuses radiation in the end-fire direction.<br>**Parameters:** Gain, directivity, size<br>**Advantages:** Improves directivity and hence gain<br>**Disadvantages:** For better gain parasitic patch should be of larger size which increases antenna size | [105], [106]<br>[107], [108] |
| Dielectric Lens | **Trivial Point:** It helps to radiate the signal in the end-fire direction, permittivity of lens should be more than substrate permittivity<br>**Parameters:** Gain, size, radiation pattern, front to back ratio, beam tilt<br>**Advantages:** Enhancement in gain, improves symmetry of radiation pattern, stable radiation pattern, high front to back ratio, reduces beam tilting at higher frequencies<br>**Disadvantages:** Increases AVA size and cost | [22], [68]<br>[69], [109] |
| Balanced AVA | **Trivial point:** It balances loading of dielectric material in between conductor and ground plane<br>**Parameters:** Beam squint, front to back ratio, gain, side lobe level(SLL), cross polarization<br>**Advantages:** Reduced beam squint, high front to back ratio, low SLL, enhanced gain, minimized cross polarization<br>**Disadvantages:** Costly, complex in design | [11], [54]<br>[78], [110]<br>[111] |
| Meta-material | **Trivial point:** Metamaterial are used in an antenna design due to their special electromagnetic characteristics which cannot be found in natural materials.<br>**Parameter:** Bandwidth, lower cut-off frequency, gain, return loss<br>**Advantages:** Reduces lower cut-off frequency and hence increases bandwidth, improves gain, reduces return loss<br>**Disadvantage:** Complex design | [9], [13]<br>[28], [46]<br>[112] |
| AVA Array | **Trivial point:** If single antenna cannot fullfill system requirements, antenna array is used.<br>**Parameters:** Gain, mutual coupling, return loss, input impedance, size<br>**Advantages:** Gain enhancement, input impedance increases, improvement in return loss<br>**Disadvantages:** Increase in antenna size, feeding network design is complex, more sidelobes, introduces mutual coupling | [88], [113]<br>[114], [115]<br>[116] |
| Computational Intelligence | **Trivial point:** It gives optimum trade offs between two or more AVA parameters<br>**Parameters:** Dimensions, beamwidth, side lobe level, reflection coefficient, lower cut-off frequency, transient distortion<br>**Advantages:** Gain enhancement, compact antenna, low SLL, improved return loss<br>**Disadvantages:** More time required for the execution of CI algorithm, programming of CI technique is complex | [24], [27]<br>[89], [90] |
| SIW | **Trivial point:** It reduces losses at higher frequencies as it resembles the characteristics of the metallic waveguide.<br>**Parameters:** Radiation loss, side lobe level, gain, isolation<br>**Advantages:** Gain enhancement, low SLL, improved isolation of array elements, low radiation loss<br>**Disadvantages:** Design complexity is higher | [19], [75]<br>[86], [87] |

techniques to verify their role in the AVA parameter enhancement.

Figure 29(a) shows the simulated S11 of designed AVA. It shows that the FR4 substrate improves return loss as compared to RO 4003 and RT/duroid 5880. Also, after incorporating corrugation, patch or dielectric lens, the return loss of AVA is improved. Further, for the same substrate (RT/duroid 5880) corrugation enhances the return loss as compared to patch and dielectric lens.

Figure 29 (b and c) are the plot of E and H plane at 27 GHz for all designed AVA. Figure 29(b) shows that the FR4 cannot enhance the gain of AVA and RT/duroid 5880 provides better gain than RO 4003. Further after incorporating dielectric lens and parasitic patch, the gain of AVA is slightly

**TABLE 13.** The comparison of all simulated AVA designs.

| S.N. | Enhancement Technique | Dimensions ($mm^3$) | Gain (dB) | Return Loss (dB) | Remarks |
|---|---|---|---|---|---|
| 1 | FR4 Substrate | 24 x 50 x 1 | 1.95 | -35.74 | Improves S11 |
| 2 | RO 4003 Substrate | 24 x 50 x 1 | 6.84 | -28.58 | Better S11 and gain |
| 3 | RT/Duroid 5880 Substrate | 24 x 50 x 1 | 10.93 | -21.94 | Best Gain |
| 4 | Parasitic Patch | 24 x 50 x 1 | 11.03 | -23.37 | Improves S11 and gain |
| 5 | Dielectric Lens | 24 x 61 x 1 | 11.14 | -22.04 | Improves S11 and gain |
| 6 | Corrugations | 24 x 50 x 1 | 11.66 | -24.91 | Improves S11 and gain and it better than other methods. |

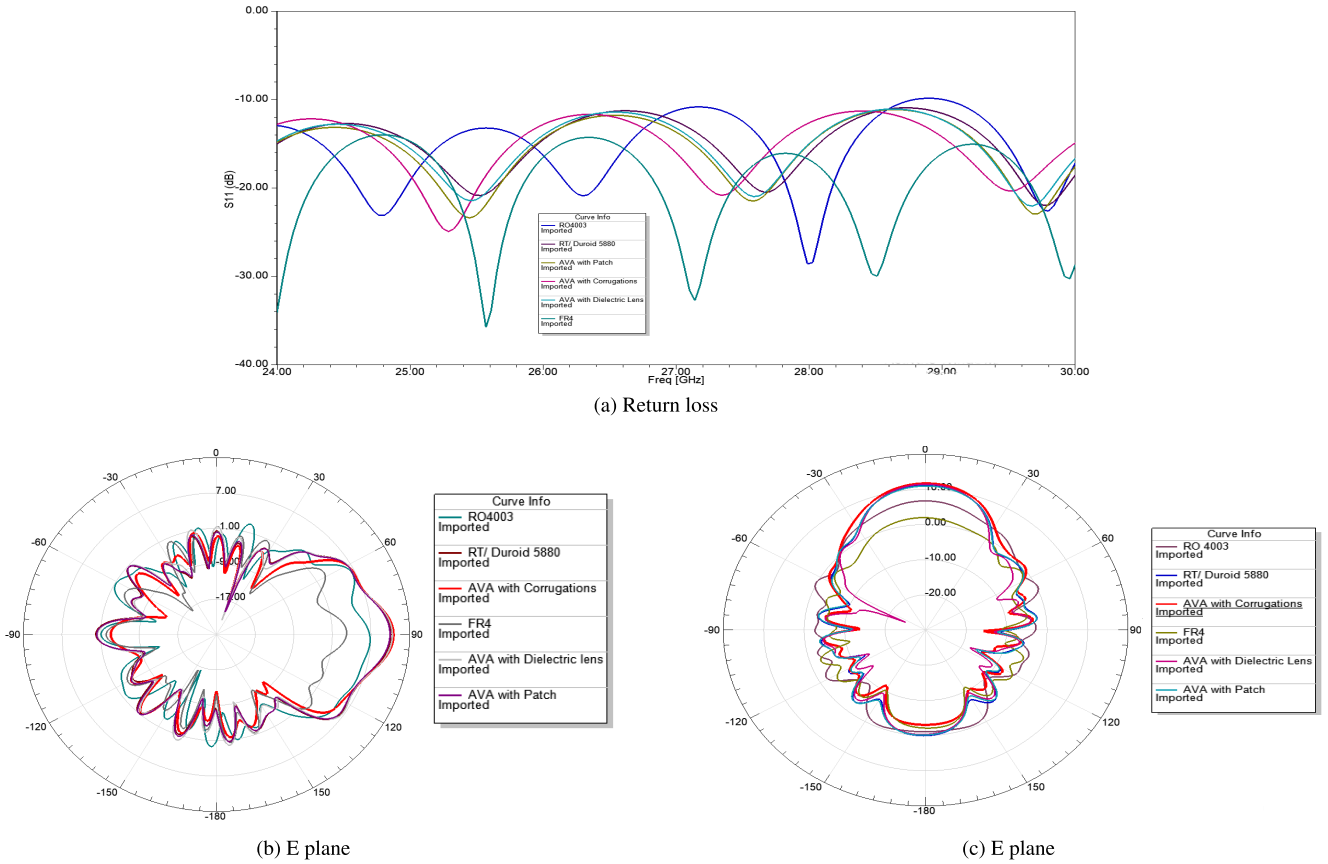


(a) Return loss

(b) E plane

(c) E plane

**FIGURE 29.** Simulated results of the designed AVA.

increased whereas after incorporating corrugation, the gain is increased by 1 dB and sidelobe levels are reduced significantly. Table 13 gives the comparison of all simulated AVA designs which explains which enhancement technique should be used according to the applications and requirements.

## IV. CONCLUSION

Antipodal Vivaldi antenna (AVA) is becoming popular in almost all wireless devices because it provides enhanced gain, wide bandwidth, improved return loss, good front to back ratio, minimum sidelobe level, and low cross-polarization. We have given a comprehensive review of all AVA performance enhancement methods present in the literature. We started with the application of AVA, its advantages, AVA design and then elaborated on each performance enhancement method. To explain each AVA enhancement method, many illustrations are listed. Different enhancement methods create a profound effect on AVA parameters. Next, we discussed various AVA performance enhancement methods reported in the literature and they are analyzed based on the improvement of AVA parameters. All these methods are explained by incorporating their importance, antenna parameters affected, their merits and demerits. These methods are based on the change in the physical geometry of an antenna which results in a change in various antenna parameters like size, gain, front to back ratio, bandwidth, radiation pattern, polarization, and operating frequency range. Each technique is discussed in detail with the help of recent research work to demonstrate the effect of a particular technique on antenna parameters. This review work demonstrates that a substrate

of low loss tangent and low permittivity must be selected to achieve enhanced gain and improved return loss. Also, AVA flare structure should be selected to make AVA more compact with all other acceptable performance parameters. Further, this review works concludes that AVA performance enhancement methods like slots, corrugation, dielectric lens, and BAVA can be used to eradicate the adverse effect of beam squint and cross-polarization. Similarly, the parasitic patch and dielectric lens should be designed such that it will focus maximum radiation in the end-fire direction to maximize the gain. Moreover, the design of a unit cell of metamaterial is the challenging task and it should be carefully designed and positioned on AVA to enhance its gain, bandwidth and return loss. In a multi-objective optimization tread-off, the researcher can employ suitable CI technique. In the applications where antenna radiation losses are more important, SIW can be employed in the feeding network to take the advantages of metallic waveguide. Additionally, to validate the performance enhancement methods, they are simulated using a basic conventional AVA which substantiates the surveyed literature results. As this survey enlighten all AVA performance enhancement methods, this survey will serve as guidelines and reference to new researchers to appropriately select the AVA performance enhancement technique while designing an antenna for a particular application.

## REFERENCES

[1] P. Gibson, "The Vivaldi aerial," in *Proc. 9th Eur. Microw. Conf.*, vol. 1, 1979, pp. 101–105.

[2] D. Schaubert, E. Kollberg, T. Korzeniowski, T. Thungren, J. Johansson, and K. Yngvesson, "Endfire tapered slot antennas on dielectric substrates," *IEEE Trans. Antennas Propag.*, vol. AP-33, no. 12, pp. 1392–1400, Dec. 1985.

[3] E. Gazit, "Improved design of the Vivaldi antenna," *IEE Proc. H Microw., Antennas Propag.*, vol. 135, no. 2, p. 89, 1988.

[4] D. Yang, S. Liu, and D. Geng, "A miniaturized ultra-wideband Vivaldi antenna with low cross polarization," *IEEE Access*, vol. 5, pp. 23352–23357, 2017.

[5] M.-A. Boujemaa, R. Herzi, F. Choubani, and A. Gharsallah, "UWB antipodal Vivaldi antenna with higher radiation performances using metamaterials," *Appl. Phys. A, Solids Surf.*, vol. 124, no. 10, pp. 1–7, Sep. 2018, doi: 10.1007/s00339-018-2132-1.

[6] Z. Tahar, D. Xavier, and M. Benslama, "An ultra-wideband modified Vivaldi antenna applied to ground and through the wall imaging," *Prog. Electromagn. Res.*, vol. 86, pp. 111–122, Aug. 2018.

[7] M. Moosazadeh, "High-gain antipodal Vivaldi antenna surrounded by dielectric for wideband applications," *IEEE Trans. Antennas Propag.*, vol. 66, no. 8, pp. 4349–4352, Aug. 2018.

[8] N. Tiwari and T. Rama Rao, "Substrate integrated waveguide based high gain planar antipodal linear tapered slot antenna with dielectric loading for 60 GHz communications," *Wireless Pers. Commun.*, vol. 97, no. 1, pp. 1385–1400, Jun. 2017.

[9] S. El-Nady, H. M. Zamel, M. Hendy, A. H. A. Zekry, and A. M. Attiya, "Gain enhancement of a millimeter wave antipodal Vivaldi antenna by epsilon-near-zero metamaterial," *Prog. Electromagn. Res.*, vol. 85, no. 1, pp. 105–116, 2018.

[10] M. Moosazadeh and S. Kharkovsky, "A compact high-gain and Front-to-Back ratio elliptically tapered antipodal Vivaldi antenna with trapezoid-shaped dielectric lens," *IEEE Antennas Wireless Propag. Lett.*, vol. 15, pp. 552–555, 2016.

[11] N.-N. Wang, M. Fang, H.-T. Chou, J.-R. Qi, and L.-Y. Xiao, "Balanced antipodal Vivaldi antenna with asymmetric substrate cutout and dual-scale slotted edges for ultrawideband operation at millimeter-wave frequencies," *IEEE Trans. Antennas Propag.*, vol. 66, no. 7, pp. 3724–3729, Jul. 2018.

[12] Z. Yang, H. Jingjian, W. Weiwei, and Y. Naichang, "An antipodal Vivaldi antenna with band-notched characteristics for ultra-wideband applications," *AEU Int. J. Electron. Commun.*, vol. 76, pp. 152–157, Jun. 2017, doi: 10.1016/j.aeue.2017.03.026.

[13] G.-N. Tan, X.-X. Yang, Z.-L. Lu, and X.-S. Jiang, "Metamaterial loaded Vivaldi antenna with high gain and equal beamwidths at KA band," *Microw. Opt. Technol. Lett.*, vol. 58, no. 10, pp. 2337–2341, Jul. 2016.

[14] F. Etesami, S. Khorshidi, S. Shahcheraghi, and A. Yahaghi, "Improvement of radiation characteristics of balanced antipodal Vivaldi antenna using trasformation optics," *Prog. Electromagn. Res.*, vol. 56, no. 1, pp. 189–196, 2017.

[15] M. Moosazadeh, S. Kharkovsky, J. T. Case, and B. Samali, "Improved radiation characteristics of small antipodal Vivaldi antenna for microwave and millimeter-wave imaging applications," *IEEE Antennas Wireless Propag. Lett.*, vol. 16, pp. 1961–1964, 2017.

[16] A. Dadgarpour, F. Jolani, Y. Yu, Z. Chen, B. S. Virdee, and T. A. Denidni, "A compact balanced antipodal bow-tie antenna having double notch-bands," *Microw. Opt. Technol. Lett.*, vol. 56, no. 9, pp. 2010–2014, Jun. 2014.

[17] X. Zhang, Y. Chen, M. Tian, J. Liu, and H. Liu, "A compact wide-band antipodal Vivaldi antenna design," *Int. J. RF Microw. Comput.-Aided Eng.*, vol. 29, no. 4, Oct. 2018, Art. no. e21598.

[18] A. Molaei, M. Kaboli, M. S. Abrishamian, and S. A. Mirtaheri, "Dielectric lens balanced antipodal Vivaldi antenna with low cross-polarisation for ultra-wideband applications," *IET Microw., Antennas Propag.*, vol. 8, no. 14, pp. 1137–1142, Nov. 2014.

[19] M. J. Horst, M. T. Ghasr, and R. Zoughi, "Design of a compact V-band transceiver and antenna for millimeter-wave imaging systems," *IEEE Trans. Instrum. Meas.*, vol. 68, no. 11, pp. 4400–4411, Nov. 2019.

[20] T. Goel and A. Patnaik, "Novel broadband antennas for future mobile communications," *IEEE Trans. Antennas Propag.*, vol. 66, no. 5, pp. 2299–2308, May 2018.

[21] M. Moosazadeh, J. T. Case, and S. Kharkovsky, "Microwave and millimetre wave antipodal Vivaldi antenna with trapezoid-shaped dielectric lens for imaging of construction materials," *IET Microw., Antennas Propag.*, vol. 10, no. 3, pp. 301–309, Feb. 2016.

[22] D. Huang, H. Yang, Y. Wu, F. Zhao, and X. Liu, "A high-gain antipodal Vivaldi antenna with multi-layer planar dielectric lens," *J. Electromagn. Waves Appl.*, vol. 32, no. 4, pp. 403–412, Oct. 2017, doi: 10.1080/09205071.2017.1393350.

[23] M. Moosazadeh, S. Kharkovsky, J. T. Case, and B. Samali, "Antipodal Vivaldi antenna with improved radiation characteristics for civil engineering applications," *IET Microw., Antennas Propag.*, vol. 11, no. 6, pp. 796–803, 2017.

[24] S. Chamaani, S. A. Mirtaheri, and M. S. Abrishamian, "Improvement of time and frequency domain performance of antipodal Vivaldi antenna using multi-objective particle swarm optimization," *IEEE Trans. Antennas Propag.*, vol. 59, no. 5, pp. 1738–1742, May 2011.

[25] A. Revna, L. I. Balderas, and M. A. Panduro, "4D antenna array of UWB Vivaldi elements with low side lobes and harmonic suppresion," in *Proc. IEEE Int. Symp. Antennas Propag. USNC/URSI Nat. Radio Sci. Meeting*, Jul. 2018, pp. 1505–1506.

[26] A. Reyna and L. I. Balderas, "Time-domain design of a linear antenna array for wideband shaped beams," in *Proc. IEEE Int. Symp. Antennas Propag. USNC/URSI Nat. Radio Sci. Meeting*, Jul. 2017, pp. 2109–2110.

[27] F. Jolani, G. R. Dadashzadeh, M. Naser-Moghadasi, and A. M. Dadgarpour, "Design and optimization of compact balanced antipodal Vivaldi antenna," *Prog. Electromagn. Res.*, vol. 9, no. 1, pp. 183–192, 2009.

[28] A. R. H. Alhawari, A. Ismail, M. A. Mahdi, and R. S. A. R. Abdullah, "Antipodal Vivaldi antenna performance booster exploiting snug-in negative index metamaterial," *Prog. Electromagn. Res.*, vol. 27, no. 1, pp. 265–279, 2012.

[29] S. Zhu, H. Liu, Z. Chen, and P. Wen, "A compact gain-enhanced Vivaldi antenna array with suppressed mutual coupling for 5G mmWave application," *IEEE Antennas Wireless Propag. Lett.*, vol. 17, no. 5, pp. 776–779, May 2018.

[30] R.-C. Deng, X.-M. Yang, B. Ma, T.-Q. Li, H.-Y. Chen, Y. Yang, H. He, Y.-W. Chen, and Z. Tang, "Performance enhancement of novel antipodal Vivaldi antenna with irregular spacing distance slots and modified-w-shaped metamaterial loading," *Appl. Phys. A, Solids Surf.*, vol. 125, no. 1, pp. 1–11, Dec. 2018, doi: 10.1007/s00339-018-2298-6.

[31] S. Zhu, H. Liu, and P. Wen, "A new method for achieving miniaturization and gain enhancement of Vivaldi antenna array based on anisotropic metasurface," *IEEE Trans. Antennas Propag.*, vol. 67, no. 3, pp. 1952–1956, Mar. 2019.
[32] A. Ghiotto, F. Parment, T.-P. Vuong, and K. Wu, "Millimeter-wave air-filled SIW antipodal linearly tapered slot antenna," *IEEE Antennas Wireless Propag. Lett.*, vol. 16, pp. 768–771, 2017.
[33] A. Gorai, A. Karmakar, M. Pal, and R. Ghatak, "A super wideband chebyshev tapered antipodal Vivaldi antenna," *AEU-Int. J. Electron. Commun.*, vol. 69, no. 9, pp. 1328–1333, Sep. 2015, doi: 10.1016/j.aeue.2015.05.017.
[34] S. Lee, J. Hur, M.-B. Heo, S. Kim, H. Choo, and G. Byun, "A suboptimal approach to antenna design problems with kernel regression," *IEEE Access*, vol. 7, pp. 17461–17468, 2019.
[35] B. Biswas, R. Ghatak, and D. R. Poddar, "A fern fractal leaf inspired wideband antipodal Vivaldi antenna for microwave imaging system," *IEEE Trans. Antennas Propag.*, vol. 65, no. 11, pp. 6126–6129, Nov. 2017.
[36] L. Li, X. Xia, Y. Liu, and T. Yang, "Wideband balanced antipodal Vivaldi antenna with enhanced radiation parameters," *Prog. Electromagn. Res.*, vol. 66, no. 1, pp. 163–171, 2016.
[37] A. M. de Oliveira, J. F. Justo, M. B. Perotoni, S. T. Kofuji, A. G. Neto, R. C. Bueno, and H. Baudrand, "A high directive koch fractal Vivaldi antenna design for medical near-field microwave imaging applications," *Microw. Opt. Technol. Lett.*, vol. 59, no. 2, pp. 337–346, Dec. 2016.
[38] A. Muniyasamy and K. Rajakani, "UWB radar cross section reduction in a compact antipodal Vivaldi antenna," *AEU-Int. J. Electron. Commun.*, vol. 99, pp. 369–375, Feb. 2019, doi: 10.1016/j.aeue.2018.12.020.
[39] J. Bai, S. Shi, and D. W. Prather, "Modified compact antipodal Vivaldi antenna for 4–50-GHz UWB application," *IEEE Trans. Microw. Theory Techn.*, vol. 59, no. 4, pp. 1051–1057, Apr. 2011.
[40] J. Eichenberger, E. Yetisir, and N. Ghalichechian, "High-gain antipodal Vivaldi antenna with pseudoelement and notched tapered slot operating at (2.5 to 57) GHz," *IEEE Trans. Antennas Propag.*, vol. 67, no. 7, pp. 4357–4366, Jul. 2019.
[41] L. Juan, F. Guang, Y. Lin, and F. Demin, "A modified balanced antipodal Vivaldi antenna with improved radiation characteristics," *Microw. Opt. Technol. Lett.*, vol. 55, no. 6, pp. 1321–1325, Mar. 2013.
[42] I. T. Nassar and T. M. Weller, "A novel method for improving antipodal Vivaldi antenna performance," *IEEE Trans. Antennas Propag.*, vol. 63, no. 7, pp. 3321–3324, Jul. 2015.
[43] F. Guangyou, "New design of the antipodal Vivaldi antenna for a GPR system," *Microw. Opt. Technol. Lett.*, vol. 44, no. 2, pp. 136–139, 2004.
[44] H. Liu, W. Yang, A. Zhang, S. Zhu, Z. Wang, and T. Huang, "A miniaturized gain-enhanced antipodal Vivaldi antenna and its array for 5G communication applications," *IEEE Access*, vol. 6, pp. 76282–76288, 2018.
[45] F. Abayaje and P. Febvre, "A customized reduced size antipodal Vivaldi antenna used in wireless baseband transmission for short-range communication," *AEU-Int. J. Electron. Commun.*, vol. 70, no. 12, pp. 1684–1691, Dec. 2016, doi: 10.1016/j.aeue.2016.10.007.
[46] S. Zhu, H. Liu, P. Wen, L. Du, and J. Zhou, "A miniaturized and high gain double-slot Vivaldi antenna using wideband index-near-zero metasurface," *IEEE Access*, vol. 6, pp. 72015–72024, 2018.
[47] H. Hong, J. G. Jeong, J. Ahn, I.-J. Yoon, and Y. J. Yoon, "Miniaturized antipodal tapered slot antenna with lower frequency band extension characteristic," *Microw. Opt. Technol. Lett.*, vol. 59, no. 7, pp. 1570–1573, May 2017.
[48] Z. Esmati and M. Moosazadeh, "Reflection and transmission of microwaves in reinforced concrete specimens irradiated by modified antipodal Vivaldi antenna," *Microw. Opt. Technol. Lett.*, vol. 60, no. 9, pp. 2113–2121, Aug. 2018.
[49] A. Z. Hood, T. Karacolak, and E. Topsakal, "A small antipodal Vivaldi antenna for ultrawide-band applications," *IEEE Antennas Wireless Propag. Lett.*, vol. 7, pp. 656–660, 2008.
[50] R. Natarajan, J. V. George, M. Kanagasabai, and A. K. Shrivastav, "A compact antipodal vivaldi antenna for UWB applications," *IEEE Antennas Wireless Propag. Lett.*, vol. 14, pp. 1557–1560, 2015.
[51] X. Qing, Z. N. Chen, and M. Y. W. Chia, "Dual elliptically tapered antipodal slot antenna loaded by curved terminations for ultrawideband applications," *Radio Sci.*, vol. 41, no. 6, pp. 1–10, Dec. 2006.
[52] P. Fei, Y.-C. Jiao, W. Hu, and F.-S. Zhang, "A miniaturized antipodal Vivaldi antenna with improved radiation characteristics," *IEEE Antennas Wireless Propag. Lett.*, vol. 10, pp. 127–130, 2011.
[53] Z. Wang, Y. Yin, J. Wu, and R. Lian, "A miniaturized CPW-fed antipodal Vivaldi antenna with enhanced radiation performance for wideband applications," *IEEE Antennas Wireless Propag. Lett.*, to be published.
[54] P. Wang, H. Zhang, G. Wen, and Y. Sun, "Design of modified 6–18 GHz balanced antipodal Vivaldi antenna," *Prog. Electromagn. Res.*, vol. 25, no. 1, pp. 271–285, 2012.
[55] A. M. De Oliveira, M. B. Perotoni, S. T. Kofuji, and J. F. Justo, "A palm tree antipodal Vivaldi antenna with exponential slot edge for improved radiation pattern," *IEEE Antennas Wireless Propag. Lett.*, vol. 14, pp. 1334–1337, 2015.
[56] M. A. Ashraf, I. Memon, and S. A. Alshebeili, "Design and analysis of broadband antipodal Vivaldi antenna for radio over fiber systems," *Microw. Opt. Technol. Lett.*, vol. 59, no. 6, pp. 1441–1446, Mar. 2017.
[57] M. Moosazadeh, S. Kharkovsky, J. T. Case, and B. Samali, "UWB antipodal Vivaldi antenna for microwave imaging of construction materials and structures," *Microw. Opt. Technol. Lett.*, vol. 59, no. 6, pp. 1259–1264, Mar. 2017.
[58] P. Ludlow and V. F. Fusco, "Antipodal Vivaldi antenna with tuneable band rejection capability," *IET Microw., Antennas Propag.*, vol. 5, no. 3, pp. 372–378, 2011.
[59] J. Y. Siddiqui, C. Saha, C. Sarkar, L. A. Shaik, and Y. M. M. Antar, "Ultra-wideband antipodal tapered slot antenna with integrated frequency-notch characteristics," *IEEE Trans. Antennas Propag.*, vol. 66, no. 3, pp. 1534–1539, Mar. 2018.
[60] R. Natarajan, M. Kanagasabai, and M. Gulam Nabi Alsath, "Dual mode antipodal Vivaldi antenna," *IET Microw., Antennas Propag.*, vol. 10, no. 15, pp. 1643–1647, Dec. 2016.
[61] Z. Briqech, A. Sebak, and T. A. Denidni, "High gain 60 GHz antipodal Fermi tapered slot antenna with sine corrugation," *Microw. Opt. Technol. Lett.*, vol. 57, no. 1, pp. 6–9, Nov. 2014.
[62] K. D. Phalak, Z. Briqech, and A. Sebak, "Ka-band antipodal Fermi-linear tapered slot antenna with a knife edge corrugation," *Microw. Opt. Technol. Lett.*, vol. 57, no. 2, pp. 485–489, Dec. 2014.
[63] X. S. Loo, M. Z. Win, and K. S. Yeo, "A high gain 60 GHz antipodal Fermi-tapered slot antenna based on robust synthesized dielectric," *Microw. Opt. Technol. Lett.*, vol. 61, no. 3, pp. 761–765, Dec. 2018.
[64] D.-M. In, M.-J. Lee, D. Kim, C.-Y. Oh, and Y.-S. Kim, "Antipodal linearly tapered slot antenna using unequal half-circular defected sides for gain improvements," *Microw. Opt. Technol. Lett.*, vol. 54, no. 8, pp. 1963–1965, May 2012.
[65] Z. Li, X. Kang, J. Su, Q. Guo, Y. Yang, and J. Wang, "A wideband end-fire conformal Vivaldi antenna array mounted on a dielectric cone," *Int. J. Antennas Propag.*, vol. 2016, Aug. 2016, Art. no. 9812642.
[66] J. Bang, J. Lee, and J. Choi, "Design of a wideband antipodal Vivaldi antenna with an asymmetric parasitic patch," *J. Electromagn. Eng. Sci.*, vol. 18, no. 1, pp. 29–34, Jan. 2018.
[67] K. Yang, M.-H. Hoang, X. Bao, P. McEvoy, and M. J. Ammann, "Dual-stub ka-band Vivaldi antenna with integrated bandpass filter," *IET Microw., Antennas Propag.*, vol. 12, no. 5, pp. 668–671, Apr. 2018.
[68] J. Bourqui, M. Okoniewski, and E. C. Fear, "Balanced antipodal Vivaldi antenna with dielectric director for near-field microwave imaging," *IEEE Trans. Antennas Propag.*, vol. 58, no. 7, pp. 2318–2326, Jul. 2010.
[69] M. Amiri, F. Tofigh, A. Ghafoorzadeh-Yazdi, and M. Abolhasan, "Exponential antipodal vivaldi antenna with exponential dielectric lens," *IEEE Antennas Wireless Propag. Lett.*, vol. 16, pp. 1792–1795, 2017.
[70] K. Kota and L. Shafai, "Gain and radiation pattern enhancement of balanced antipodal Vivaldi antenna," *Electron. Lett.*, vol. 47, no. 5, p. 303, 2011.
[71] X. Li, Y. Xu, H. Wang, Y. Zhang, and G. Lv, "Low cross-polarization antipodal tapered slot antenna with gain bandwidth enhancement for UWB application," *J. Comput. Electron.*, vol. 17, no. 1, pp. 442–451, Oct. 2017.
[72] M. Moosazadeh, S. Kharkovsky, J. T. Case, and B. Samali, "Miniaturized UWB antipodal Vivaldi antenna and its application for detection of void inside concrete specimens," *IEEE Antennas Wireless Propag. Lett.*, vol. 16, pp. 1317–1320, 2017.
[73] Y. Zhang, E. Li, C. Wang, and G. Guo, "Radiation enhanced Vivaldi antenna with double-antipodal structure," *IEEE Antennas Wireless Propag. Lett.*, vol. 16, pp. 561–564, 2017.
[74] G. Teni, N. Zhang, J. Qiu, and P. Zhang, "Research on a novel miniaturized antipodal Vivaldi antenna with improved radiation," *IEEE Antennas Wireless Propag. Lett.*, vol. 12, pp. 417–420, 2013.

[75] R. Kazemi, A. E. Fathy, and R. A. Sadeghzadeh, "Dielectric rod antenna array with substrate integrated waveguide planar feed network for wideband applications," *IEEE Trans. Antennas Propag.*, vol. 60, no. 3, pp. 1312–1319, Mar. 2012.

[76] F. Wan, J. Chen, and B. Li, "A novel ultra-wideband antipodal Vivaldi antenna with trapezoidal dielectric substrate," *Microw. Opt. Technol. Lett.*, vol. 60, no. 2, pp. 449–455, Jan. 2018.

[77] M. Moosazadeh and S. Kharkovsky, "Development of the antipodal Vivaldi antenna for detection of cracks inside concrete members," *Microw. Opt. Technol. Lett.*, vol. 57, no. 7, pp. 1573–1578, Apr. 2015.

[78] C. Sarkar, C. Saha, L. A. Shaik, J. Y. Siddiqui, and Y. M. M. Antar, "Frequency notched balanced antipodal tapered slot antenna with very low cross-polarised radiation," *IET Microw., Antennas Propag.*, vol. 12, no. 11, pp. 1859–1863, Sep. 2018.

[79] R. Singha and D. Vakula, "Corrugated antipodal Vivaldi antenna using spiral shape negative index metamaterial for ultra-wideband application," in *Proc. Int. Conf. Signal Process. Commun. Eng. Syst.*, Jan. 2015, pp. 179–183.

[80] M. Sun, Z. N. Chen, and X. Qing, "Gain enhancement of 60-GHz antipodal tapered slot antenna using zero-index metamaterial," *IEEE Trans. Antennas Propag.*, vol. 61, no. 4, pp. 1741–1746, Apr. 2013.

[81] X. Li, H. Zhou, Z. Gao, H. Wang, and G. Lv, "Metamaterial slabs covered UWB antipodal Vivaldi antenna," *IEEE Antennas Wireless Propag. Lett.*, vol. 16, pp. 2943–2946, 2017.

[82] B. Tütüncu, H. Torpi, and B. Urul, "A comparative study on different types of metamaterials for enhancement of microstrip patch antenna directivity at the Ku-band (12 GHz)," *Turkish J. Electr. Eng. Comput. Sci.*, vol. 26, no. 3, pp. 1171–1179, 2018.

[83] J. D. S. Langley, P. S. Hall, and P. Newham, "Balanced antipodal Vivaldi antenna for wide bandwidth phased arrays," *IEE Proc.-Microw., Antennas Propag.*, vol. 143, no. 2, p. 97, 1996.

[84] L. Guo and Y. F. Qiang, "Design of a compact wideband dual-polarization antipodal Vivaldi antenna array," in *Proc. IEEE Int. Conf. Comput. Electromagn. (ICCEM)*, Mar. 2018, pp. 1–3.

[85] S. S. Holland and M. N. Vouvakis, "The banyan tree antenna array," *IEEE Trans. Antennas Propag.*, vol. 59, no. 11, pp. 4060–4070, Nov. 2011.

[86] H.-Q. Ma and T. Feng, "Antipodal linearly tapered slot antenna with reduced mutual coupling fed by substrate integrated waveguide," *Microw. Opt. Technol. Lett.*, vol. 53, no. 11, pp. 2512–2515, Aug. 2011.

[87] S. Gupta, Z. Briqech, and A. R. Sebak, "Substrate integrated-based Fermi-dirac multibeam antenna for mmWave applications," *Electron. Lett.*, vol. 53, no. 19, pp. 1318–1319, Sep. 2017.

[88] W. Shao and R. S. Adams, "Two antipodal Vivaldi antennas and an antenna array for microwave early breast cancer detection," *Microw. Opt. Technol. Lett.*, vol. 55, no. 3, pp. 670–674, Jan. 2013.

[89] S. Chamaani, M. S. Abrishamian, and S. A. Mirtaheri, "Time-domain design of UWB Vivaldi antenna array using multiobjective particle swarm optimization," *IEEE Antennas Wireless Propag. Lett.*, vol. 9, pp. 666–669, 2010.

[90] M. A. Pumallica-Paro, J. L. Arizaca-Cusicuna, and M. Clemente-Arenas, "A multiobjective genetic algorithm for analysis, design and optimization of antipodal Vivaldi antennas," in *Proc. IEEE-APS Topical Conf. Antennas Propag. Wireless Commun. (APWC)*, Sep. 2019, pp. 316–321.

[91] M. Movahhedi, M. Karimipour, and N. Komjani, "Multibeam bidirectional wideband/wide-scanning-angle holographic leaky-wave antenna," *IEEE Antennas Wireless Propag. Lett.*, vol. 18, no. 7, pp. 1507–1511, Jul. 2019.

[92] X.-X. Li, B.-J. Lu, L. Sang, Y.-M. Zhang, and G.-Q. Lv, "Radiation enhanced Vivaldi antenna with shaped dielectric cover," *Microw. Opt. Technol. Lett.*, vol. 59, no. 8, pp. 1975–1983, May 2017.

[93] A. M. Abbosh, H. K. Kan, and M. E. Bialkowski, "Compact ultra-wideband planar tapered slot antenna for use in a microwave imaging system," *Microw. Opt. Technol. Lett.*, vol. 48, no. 11, pp. 2212–2216, 2006.

[94] D. Gaetano, M. J. Ammann, P. McEvoy, M. John, L. Keating, and F. Horgan, "Proximity study of a conformal UWB directional antenna on water pipe," *Microw. Opt. Technol. Lett.*, vol. 54, no. 8, pp. 1982–1986, May 2012.

[95] J. Wu, Z. Zhao, and Q.-H. Liu, "A novel Vivaldi antenna with extended ground plane stubs for ultrawideband applications," *Microw. Opt. Technol. Lett.*, vol. 57, no. 4, pp. 983–987, Feb. 2015.

[96] G. Ruvio, R. Solimene, A. D'Alterio, M. J. Ammann, and R. Pierri, "RF breast cancer detection employing a noncharacterized Vivaldi antenna and a MUSIC-inspired algorithm," *Int. J. RF Microw. Comput.-Aided Eng.*, vol. 23, no. 5, pp. 598–609, Nov. 2012.

[97] G. K. Pandey, H. Verma, and M. K. Meshram, "A compact antipodal vivaldi antenna for UWB applications," *Electron. Lett.*, vol. 51, no. 4, pp. 308–310, 2015.

[98] A. Saee Arezoomand, R. A. Sadeghzadeh, and M. Naser-Moghadasi, "Investigation and improvement of the phase-center characteristics of Vivaldi's antenna for UWB applications," *Microw. Opt. Technol. Lett.*, vol. 58, no. 6, pp. 1275–1281, Mar. 2016.

[99] J. Puskely, J. Lacik, Z. Raida, and H. Arthaber, "High-gain dielectric-loaded Vivaldi antenna for Ka-band applications," *IEEE Antennas Wireless Propag. Lett.*, vol. 15, pp. 2004–2007, 2016.

[100] A. M. de Oliveira, J. F. Justo, A. J. R. Serres, M. R. Manhani, R. H. C. Maniçoba, M. B. Perotoni, and H. Baudrand, "Ultra-directive palm tree Vivaldi antenna with 3D substrate lens for $\mu$-biological near-field microwave reduction applications," *Microw. Opt. Technol. Lett.*, vol. 61, no. 3, pp. 713–719, Dec. 2018.

[101] J. Guo, J. Tong, Q. Zhao, J. Jiao, J. Huo, and C. Ma, "An ultrawide band antipodal Vivaldi antenna for airborne GPR application," *IEEE Geosci. Remote Sens. Lett.*, vol. 16, no. 10, pp. 1560–1564, Oct. 2019.

[102] E. García, E. De Lera, and E. Rajo, "Tapered slotline antenna modification for radiation pattern improving," *Microw. Opt. Technol. Lett.*, vol. 49, no. 10, pp. 2590–2595, Jul. 2007.

[103] W. Mazhar, D. Klymyshyn, and A. Qureshi, "Log periodic slot-loaded circular Vivaldi antenna for 5-40 GHz UWB applications," *Microw. Opt. Technol. Lett.*, vol. 59, no. 1, pp. 159–163, Nov. 2016.

[104] F. Zhu, S. Gao, A. T. S. Ho, C. H. See, R. A. Abd-Alhameed, J. Li, and J. Xu, "Compact-size linearly tapered slot antenna for portable ultra-wideband imaging systems," *Int. J. RF Microw. Comput.-Aided Eng.*, vol. 23, no. 3, pp. 290–299, Aug. 2012.

[105] C. Gao, E. Li, Y. Zhang, and G. Guo, "A directivity enhanced structure for the Vivaldi antenna using coupling patches," *Microw. Opt. Technol. Lett.*, vol. 60, no. 2, pp. 418–424, Jan. 2018.

[106] M. Samsuzzaman, M. T. Islam, A. A. S. Shovon, R. I. Faruque, and N. Misran, "A 16-modified antipodal Vivaldi antenna array for microwave-based breast tumor imaging applications," *Microw. Opt. Technol. Lett.*, vol. 61, no. 9, pp. 2110–2118, Jun. 2019.

[107] S. Kibria, M. Samsuzzaman, M. T. Islam, M. Z. Mahmud, and N. Misran, "Breast phantom imaging using iteratively corrected coherence factor delay and sum," *IEEE Access*, vol. 7, pp. 40822–40832, 2019.

[108] P. Zhang and W.-X. Zhang, "Improved tapered slot-line antennas by using grating loading," *Microw. Opt. Technol. Lett.*, vol. 52, no. 3, pp. 728–731, Mar. 2010.

[109] X. Li, G. Liu, Y. Zhang, L. Sang, and G. Lv, "A compact multi-layer phase correcting lens to improve directive radiation of Vivaldi antenna," *Int. J. RF Microw. Comput.-Aided Eng.*, vol. 27, no. 7, Apr. 2017, Art. no. e21109.

[110] E. Guillanton, J. Y. Dauvignac, C. Pichot, and J. Cashman, "A new design tapered slot antenna for ultra-wideband applications," *Microw. Opt. Technol. Lett.*, vol. 19, no. 4, pp. 286–289, Nov. 1998.

[111] J. D. S. Langley, P. S. Hall, and P. Newham, "Novel ultrawide-bandwidth Vivaldi antenna with low crosspolarisation," *Electron. Lett.*, vol. 29, no. 23, pp. 2004–2005, 1993.

[112] S. Pandit, A. Mohan, and P. Ray, "Metamaterial-inspired low-profile high-gain slot antenna," *Microw. Opt. Technol. Lett.*, vol. 61, no. 9, pp. 2068–2073, Sep. 2019.

[113] H. Loui, J. P. Weem, and Z. Popovic, "A dual-band dual-polarized nested vivaldi slot array with multilevel ground plane," *IEEE Trans. Antennas Propag.*, vol. 51, no. 9, pp. 2168–2175, Sep. 2003.

[114] W.-H. Tu, S.-G. Kim, and K. Chang, *Wideband Microstrip-Fed Tapered Slot Antennas and Phased Array*. Hoboken, NJ, USA: Wiley, 2007, pp. 233–242.

[115] S.-G. Kim, T.-Y. Yun, and K. Chang, "Two-dimensional beam-scanning using tapered slot antennas and piezoelectric transducers," *Int. J. RF Microw. Comput.-Aided Eng.*, vol. 16, no. 4, pp. 331–337, 2006.

[116] Y. Yao, X. Cheng, C. Wang, J. Yu, and X. Chen, "Wideband circularly polarized antipodal curvedly tapered slot antenna array for 5G applications," *IEEE J. Sel. Areas Commun.*, vol. 35, no. 7, pp. 1539–1549, Jul. 2017.

**AMRUTA S. DIXIT** received the bachelor's degree in electronics and telecommunication and the master's degree in signal processing from Pune University, Pune, India, in 2008 and 2012, respectively. She is currently pursuing the Ph.D. degree with the Symbiosis Institute of Technology, Symbiosis International (Deemed University), Pune. She is currently a Junior Research Fellow at Symbiosis International (Deemed University). Her research interests include antenna design and 5G communication.

**SUMIT KUMAR** received the bachelor's degree in electronics and telecommunication from Kurukshetra University, Kurukshetra, India, in 2005, the master's degree from Guru Jambheshwar University of Science and Technology, Hisar, India, in 2008, and the Ph.D. degree from Jamia Millia Islamia, New Delhi, India, in 2017.

He is currently an Associate Professor at Electronics and Telecommunication Department, Symbiosis Institute of Technology, Symbiosis International (Deemed University), Pune, India. His research interests include antenna design, wireless networks, wireless communication, and computational intelligence.